Ludwig-Maximilians-Universität
München

Bachelor's Thesis

Spin-to-Charge Conversion in Helical Systems

Julian Christoph Thönniß

supervised by
Prof. Dr. Jan von Delft
and Dr. Oleg Yevtushenko

September 14, 2017

Ludwig-Maximilians-Universität
München

Bachelor-Arbeit

Spin-Ladungs-Konversion in Helikalen Systemen

Julian Christoph Thönniß

betreut von
Prof. Dr. Jan von Delft
and Dr. Oleg Yevtushenko

14. September, 2017

Contents

Abstract

Helical states are characterized by a lock-in-relation between spin and direction of motion. The discovery of helical states as new state of matter with virtually ideal spin- and charge transport properties have opened gates to exploring interesting new physical effects such as persistent spin currents of Dirac Fermions. It has recently been shown that helical states appear not only as edge states of topological insulators, but can also result from many-body-interaction effects in 1D quantum wires. In this thesis, we show that electron tunneling between a single-level quantum dot which is out of equilibrium (corresponding to a magnetization), and a 1D helical wire leads to spin-dependent tunneling currents. We demonstrate this to result in a spin-to-charge conversion which is an important experimental tool.
We address the problem of regularization of the tunneling Hamiltonian which always appears in the theory of 1D Dirac Fermions. By using the scattering approach and phenomenological arguments, we find a general expression for the tunneling current and analyze it for different realizations of the quantum dot.

1 Introduction

1.1 Helical States

One of the great achievements of solid states physics in the 20th century is the development of band theory that allows to describe the electronic structure of solids. At first sight, it might seem reasonable that there is no substantial difference between different insulators that have an energy gap between the valence and conduction band since one could smoothly interpolate between them by widening or narrowing the gap. Defining this as property of a topological equivalence class, this would imply that all insulators belong to the same topological class. Interestingly, there are electronic states that contradict this intuition. This topic has intensively been explored in the past decades and new states of matter have been revealed that we will discuss in this section.

1.1.1 Helical States in Topological Insulators

In 1980, von Klitzing, Dorda, and Pepper opened the gates to discovering a new phase of matter. They experimentally observed the Quantum Hall effect that arises when a strong magnetic field is applied perpendicular to a two-dimensional electron gas. The motion of a charged particle in a uniform magnetic field is equivalent to that of a simple harmonic oscillator in quantum mechanics. Thus, the electrons move on cyclotron orbits and take quantized Landau levels $\epsilon_\nu = \hbar\omega_c(\nu + 1/2)$ where $\omega_c = \frac{eB}{m}$ is the cyclotron frequency (m is the electron mass, e is the electron charge, and B is the applied magnetic field). Landau levels can be seen as band structure with level spacing $\Delta\epsilon = \hbar\omega_c$. Hence, just like an insulator, the total energy of all occupied energy levels is separated from the next higher energy state by an energy gap. It was observed that a transverse electric field causes the cyclotron orbits to drift. At the edge, the electrons are driven to perform a skipping motion since they cannot close their orbit. This skipping motion constitutes one dimensional transport channels with conductance $\frac{e^2}{h}$ per occupied level which gives rise to the quantized Hall conductivity:

$$\sigma_{xy} = \frac{Ne^2}{h}. \tag{1}$$

where N denotes the number of occupied levels. It was realized that N is in fact a topological invariant that is insensitive to the geometry of the system. In this sense, the conductivity in the Quantum Hall effect is very robust.

In 1982, Thouless, Kohmoto, Nightingale, and Nijs (TKNN) understood that the difference between ordinary insulators and Quantum Hall Insulators is in fact a matter of topology [7,23]. In order to distinguish between them, they calculated the Chern number $n_m \in \mathbb{Z}$ that can be defined in terms of Bloch wavefunctions $|u_m(\vec{k})\rangle$.

Originally, the Chern number has its roots in the mathematical theory of Fiber Bundles. The Chern number serves to classify time reversal invariant Hamiltonians of solids into topological equivalence classes according to their band structure. Two Hamiltonians of the same equivalence class can smoothly be transformed into one another without closing the energy gap between the valence and the conduction band. For the definition of n_m, a vector potential $\vec{A} := i\langle u_m(\vec{k})|\vec{\nabla}_k|u_m(\vec{k})\rangle$, called *Berry-connection*, is used. Since quantum mechanical wave functions always have an ambiguity with regard to their phase, the quantity $\vec{A}$ is not gauge invariant:

$$|u(\vec{k})\rangle \to e^{i\phi(\vec{k})}|u(\vec{k})\rangle \tag{2}$$

$$\vec{A} \to \vec{A} + \vec{\nabla}_k\phi(\vec{k}). \tag{3}$$

However, a closed path integral in k-space of the Berry connection does not contain this ambiguity, i.e. it is independent of the arbitrary phase $\phi(\vec{k})$:

$$\oint_{\mathcal{C}} d\vec{k}\, i\langle u_m(\vec{k})e^{i\phi(\vec{k})}|\vec{\nabla}_k|e^{i\phi(\vec{k})}u_m(\vec{k})\rangle \tag{4}$$

$$= \oint_{\mathcal{C}} d\vec{k}\, i\underbrace{\langle u_m(\vec{k})e^{i\phi(\vec{k})}|e^{i\phi(\vec{k})}u_m(\vec{k})\rangle}_{=1}\vec{\nabla}_k(i\phi(\vec{k})) + \oint_{\mathcal{C}} d\vec{k}\underbrace{e^{-i\phi(\vec{k})}e^{i\phi(\vec{k})}}_{=1} i\langle u_m(\vec{k})|\vec{\nabla}_k|u_m(\vec{k})\rangle \tag{5}$$

$$= 0 + \oint_{\mathcal{C}} d\vec{k}\, i\langle u_m(\vec{k})|\vec{\nabla}_k|u_m(\vec{k})\rangle. \tag{6}$$

This motivates the following definition of the Chern invariant n_m:

$$n_m \equiv \frac{1}{2\pi}\oint_{\mathcal{C}} d\vec{k}\, i\langle u_m(\vec{k})|\vec{\nabla}_k|u_m(\vec{k})\rangle. \tag{7}$$

Using Stokes' Theorem, the closed path integral can also be expressed by a surface integral over the curl of $\vec{A}$:

$$n_m = \frac{1}{2\pi}\oint_{\mathcal{C}} d\vec{k}\,\vec{A} = \frac{1}{2\pi}\oint_{\partial\mathcal{C}} d^2\vec{k}\,(\vec{\nabla}\times\vec{A}), \tag{8}$$

where $(\vec{\nabla}\times\vec{A})$ is called *Berry curvature* as introcuded by Berry in 1984 [3]. Structurally, the Berry curvature is analogous to the magnetic field that is expressed as curl of the electromagnetic vector potential.
The total Chern number n is the sum over all bands: $n = \sum_m^N n_m$. It characterizes the band structure and cannot change in smooth deformations of the Hamiltonian $H(\vec{k})$ that do not close the energy gap between the valence and conduction band. n can be shown to be equivalent to N in Eq. (1).

In return, a change of the Chern number over the interface of two materials[1] requires the gap to vanish at some point which gives rise to gapless edge states that lie inside the bulk insulating gap (see Fig. 1).

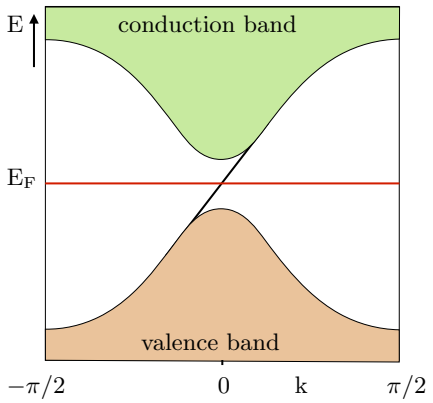

Fig. 1: Dispersion relation of a chiral edge state connecting the valence band to the conduction band.

Since, for spinless models, a topologically nontrivial bulk can only be obtained by explicitly breaking time reversal symmetry $\mathcal{T}$ (e.g. by applying a magnetic field), these edge states are chiral in the sense that electrons can only travel in one direction. The effective electric current is nonzero, accordingly. Consequently, due to the absence of states with the opposite direction of motion, back-scattering is suppressed and the edge states are immune to potential disorder.

In 1988, Haldane developed a model which gives rise to the Quantum Hall Effect: He considered a spinless graphene model which is based on a honeycomb-lattice. The corresponding Brillouin zone (BZ) is hexagonal which corresponds to a triangular Bravais lattice with a basis. One can therefore distinguish between two types of edge points: K and K'. If one expands the Hamiltonian at these points in the reciprocal lattice, the dispersion relation turns out to be linear around K and K'. Moreover, one discovers that the conductance band and the valence band touch at these points (see Fig. 2). In fact, the form of the Hamiltonian in the vicinity of K and K' is analogous to a massless Dirac Hamiltonian.

By breaking either reflection symmetry $\mathcal{R}$ or time reversal symmetry $\mathcal{T}$, a mass term can be introduced into the Dirac-Hamiltonian that lifts the degeneracy at K and K' and thus opens a band gap.
Interestingly, a broken $\mathcal{R}$-symmetry (e.g. if the two atoms in the unit cell are inequivalent) results in a trivial insulator ($n = 0$) whereas a broken $\mathcal{T}$-symmtery leads to a non-zero Chern number and therefore results in chiral edge states that are protected by symmetry. Haldane proposed a periodic magnetic flux which is zero on average to break $\mathcal{T}$-symmetry. The quantum Hall conductance is therefore not due to discrete Landau levels but originates from the band structure of electrons in the lattice.

[1] This includes the interface between a nontrivial insulator($n_m \neq 0$) and the vacuum which belongs to the trivial topological class with $n = 0$.

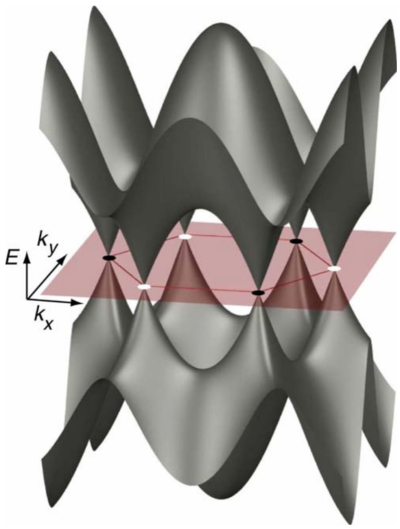

Figure 2: Three dimensional band structure of graphene. Around the two distinct edge points of the hexagonal Brillouin zone K and K', marked in black and white, the dispersion relation is linear to a good approximation, adopted from [1].

These chiral electrons with a linear dispersion relation can be described by the Dirac equation and are referred to as Dirac Fermions.

Haldane used the periodic magnetic flux to explicitly break $\mathcal{T}$-symmetry in order to obtain a topologically nontrivial bulk. One could ask whether similar states can also exist in $\mathcal{T}$-invariant systems. In 2005, Kane and Mele predicted a new phase of matter in 2D that indeed appears in $\mathcal{T}$-invariant systems and has topologically protected edge states [10]:
Up to this points, the spin of the electrons in the Haldane-graphene model was ignored. Introducing spin into the model, Kane and Mele replaced the periodic magnetic flux by spin-orbit-interaction (SOI) which respects all of gaphene's symmetries but still introduces a mass term to the Dirac Hamiltonian [10]. Spin-orbit interaction is a relativistic effect where a charged particle that travels in an electric field, experiences an effective magnetic field $\vec{B}_{\mathrm{SO}}$ that couples to its spin. The resulting model can roughly be seen as two copies of the Haldane model with opposite signs of the Hall conductivity for up and down spins [7, 10]. $\mathcal{T}$-symmetry is preserved since time reversal flips the spin as well as the sign of the conductivity. Thus, electrons with opposite spin travel in opposite directions. This state in 2D is called Quantum Spin Hall (QSH) state. Such 2D time reversal invariant insulators are also referred to as *topological insulators* which constitute a new phase of matter. Since it is two copies of a Quantum Hall state, the QSH state must have gapless edge states which are called helical due to their lock-in-relation between spin and direction of motion [7].
Generally, helicity is defined as normalized projection of a particle's spin on its

momentum:

$$h := \frac{\vec{p} \cdot \vec{s}}{|\vec{p}||\vec{s}|}.$$

In one dimension, h takes the simple form:

$$h = sgn(p)sgn(s) = \pm 1.$$

h fully characterizes a 1D helical state. This implies a lock-in relation between spin and direction of motion: Electrons of a specific spin state can only travel in one direction, whereas electrons in the other spin state always have the opposite direction of motion (see Fig. 3).

Due to SOI, the states mix and it is generally not possible to define a spin-dependent Chern number [20]. Since there is no net charge current, it is neither possible to define a total Chern number for the system. Kane and Mele therefore introduced a $\mathbb{Z}_2$ order parameter to distinguish between two classes of 2D time reversal invariant insulators [9].

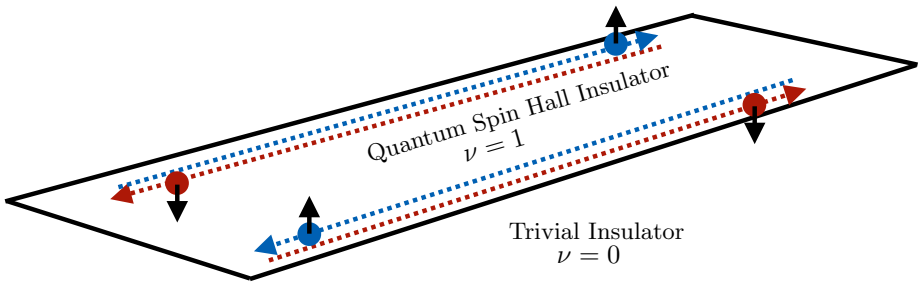

Fig. 3: Helical states that are characterized by a lock-in-relation between spin and direction of motion. Electrons with opposite spin states are counterpropagating at the edge of a Quantum Spin Hall Insulator. The $\mathbb{Z}_2$-order parameter ν is $\nu = 1$ in the bulk and $\nu = 0$ outside. Topological insulators are $\mathcal{T}$-invariant.

More insight can be gained by looking at the properties of electrons as spin-$\frac{1}{2}$-particles. The time-reversal-operator $\Theta = e^{(i\pi \hat{S}_y/\hbar)}\hat{K}$, where $\hat{S}_y$ is the spin-operator and $\hat{K}$ is complex conjugation, is antiunitary:

$$\Theta^2 = -1 \tag{9}$$

This implies that all eigenstates are at least two-fold degenerate which is known as Kramer's Theorem. This can be understood as follows: If the eigenstates of Θ

were not degenerate, one could write the eigenvalue-equation $\Theta|\chi\rangle = c|\chi\rangle$ with a constant c. This is in contradiction to $\Theta^2|\chi\rangle = -|\chi\rangle = |c|^2|\chi\rangle$ since $|c|^2 \neq -1$ and one can therefore conclude that, for spin-$\frac{1}{2}$-particles, the eigenstates of $\mathcal{T}$-invariant Hamiltonians are at least twofold degenerate.
The above assumed $\mathcal{T}$-invariance of the Hamiltonian for QSH-insulators implies that time reversal flips the spin σ and the momentum k of the Hamiltonian $H(\vec{k}_\sigma)$:

$$\Theta H(\vec{k}_\sigma)\Theta^{-1} = H(-\vec{k}_{-\sigma}). \tag{10}$$

Consequently, the one half of the Brillouin zone with negative k-values is simply a mirror image of the one with positive k-values. At the point $k = 0$ and at the edge points $k = \Gamma_b = \pm\pi/a$, the two states must cross due to their Kramer's degeneracy. At all other values of k, the degeneracy is lifted by spin-orbit-interaction.

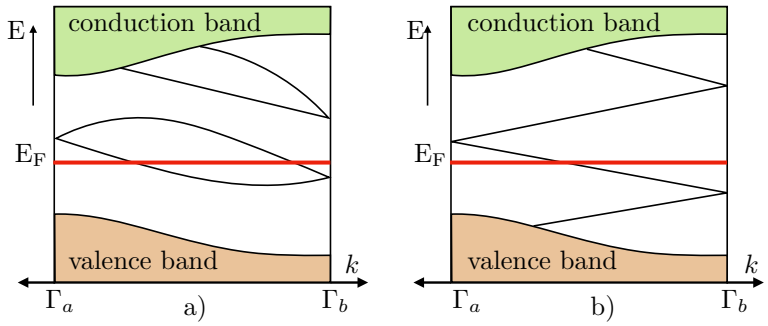

Fig. 4: Electronic dispersion between two boundary Kramer's degenerate points $\Gamma_a = 0$ and $\Gamma_b = \pi/a$. In a), the number of surface states crossing the Fermi energy E_F is even, whereas in b) it is odd. An odd number of crossings leads to topologically protected metallic boundary states, adapted from [7].

If the bands cross the Fermi energy an even number of times as depicted in Fig. 4 a), one can shift the energy in a way that all the bound states are pushed out of the gap which implies the topological equivalence to trivial insulators. If the bands intersect the Fermi energy an odd number of times, in contrast (Fig. 4 b)), shifting the energy by adding $\mathcal{T}$-invariant impurities cannot remove the degeneracy points. This insulator is therefore nontrivial and has helical edge states that are topologically protected by $\mathcal{T}$-symmetry. This essential difference between an even and an odd number of helical edge states motivates the introduction of a $\mathbb{Z}_2$ order parameter:

$$\nu \equiv \begin{cases} 0 & \text{trivial insulators (even number of crossings at } E_F) \\ 1 & \text{nontrivial insulators (odd number of crossings at } E_F) \end{cases}. \tag{11}$$

The robustness of the helical edge states is a central property that we demonstrate for a $\mathcal{T}$-invariant scattering potential V: Due to Eq. (9), it is natural to use the following convention for the time reversal operator Θ acting on a Bloch wavefunction $|u_{k,\sigma}\rangle$ with momentum k and spin σ:

$$\Theta|u_{k,\uparrow}\rangle = |u_{-k,\downarrow}\rangle \tag{12}$$

$$\Theta|u_{-k,\downarrow}\rangle = -|u_{k,\uparrow}\rangle. \tag{13}$$

The antiunitary operator Θ has the property $\langle\Theta\alpha|V|\Theta\beta\rangle = \langle\beta|V|\alpha\rangle$ for general states α and β. It follows that

$$\langle u_{k,\uparrow}|V|u_{-k,\downarrow}\rangle = \langle\Theta u_{-k,\downarrow}|V|\Theta u_{k,\uparrow}\rangle = -\langle u_{k,\uparrow}|V|u_{-k,\downarrow}\rangle, \tag{14}$$

and therefore: $\langle u_{k,\uparrow}|V|u_{-k,\downarrow}\rangle = 0$ which is the condition for robustness.

1.1.2 Helical States in Interacting Wires

In the last section, we considered only noninteracting systems where symmetry protected states were due to a topologically nontrivial bulk.
However, it was discovered that many-body interaction effects can also give rise to helical states. In 2010, Quay et al. observed that spin-orbit-interaction (SOI) in 1D wires can lead to such states by the following mechanism [14]: Due to SOI, the spin degeneracy of conduction electrons in a wire is lifted and one obtains two spinful bands. The magnetic field $\vec{B}_{\mathrm{SO}}$, which acts on electrons, is perpendicular to both, the electron's momentum and external electric field that can arise as a result of either the lack of an inversion centre in the crystal or a lack of symmetry in an external confining potential such as metallic gates. Quay et al. showed that, when an additional magnetic field is applied perpendicular to $\vec{B}_{\mathrm{SO}}$, the bands mix and the crossing points become anticrossings (see Fig. 5).

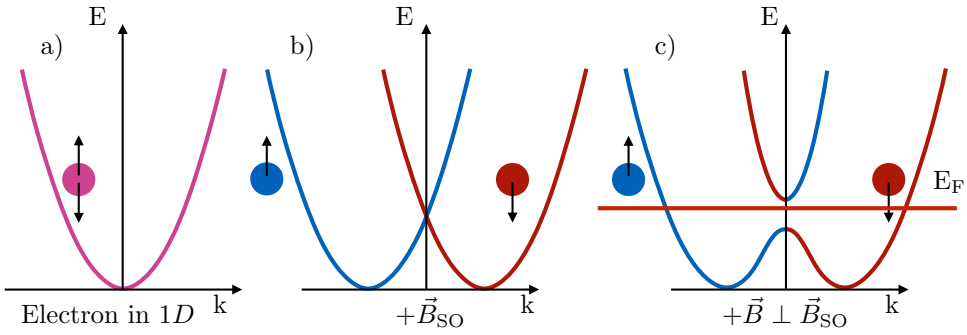

Fig. 5: a) Dispersion relation of electrons in 1D without spin-orbit interaction. b),c) Dispersion relation for different orientations of $\vec{B}$ with respect to $\vec{B}_{\mathrm{SO}}$. For $\vec{B} \perp \vec{B}_{\mathrm{SO}}$, a spin-orbit gap opens that gives rise to helical states.

If the Fermi energy lies within the so-called spin-orbit-gap of such an anticrossing point, only two states exist instead of the previous four. These two states are helical in a similar way that conducting electrons in egde states of topological insulators are helical: Backscattering requires a spin flip and therefore, the states are immune to potential disorder.

Experimentally, a one dimensional hole wire can be realized as follows: In a first step, a two-dimensional hole gas is produced in a AlGaAs/GaAs/AlGaAs quantum well. Carbon-p-doping leads to the accumulation of a high mobility 2 dimensional hole gas (2DHG) at the interface. Then, the sample is cleaved and more p-doped AlGaAs is grown over the freshly exposed surface. Applying a positive voltage at the gate electrode that is parallel to the 2DHG, one can deplete the 2DHG under the gate which results in a one dimensional hole wire as shown in Fig. 6. This fabrication technique is called cleaved-edge overgrowth method.

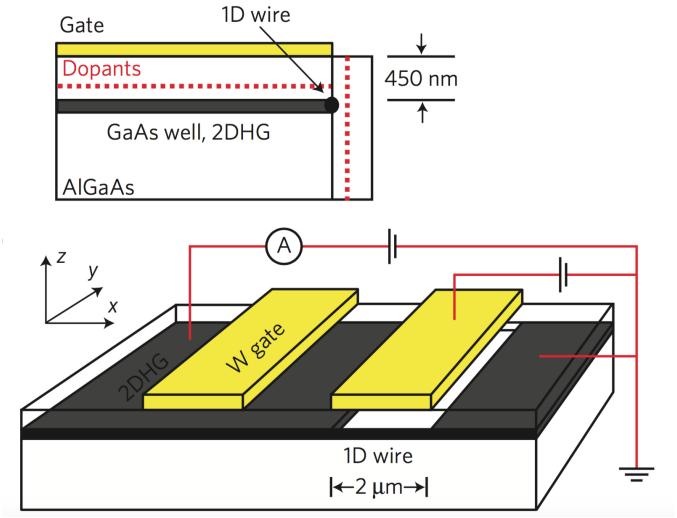

Fig. 6: Top: Cross-section of the device for the creation of 1D hole wires which is fabricated by the cleaved-edge overgrowth method. Bottom: A section of the wire is isolated using a gate which depletes the 2DHG just beneath it, adapted from [14].

Loss et al. showed in [4] that an embedded 3D nuclear spin lattice in such 1D GaAs-based quantum wires with interacting electrons leads to order in both systems in the form of a nuclear helimagnet and a helical spin density wave for half of the electron modes. The responsible mechanism is the Ruderman-Kittel-Kasuya-Yosida (RKKY)-interaction which is an indirect exchange coupling: the spin of one atom interacts with a conduction electron via hyperfine interaction and this conduction electron then interacts with another nuclear spin, thus creating a correlation energy

between the two spins.

Tsvelik and Yevtushenko showed in [24] and [19] that in interacting systems, spontaneous symmetry breaking can also give rise to helical modes. They concentrated on the RKKY-interaction in low-energy regimes of a model Kondo chain. RKKY is the dominant interaction effect when the spin concentration is large and the electron-electron-repulsion is present. The model consists of electrons that travel in one dimension and interact with localized magnetic moments.
The coupling between the eletron spins and the magnetic moments of the atomic nuclei is considered to be isotropic in the x-y-plane: $J_x = J_y = J_\perp \neq J_z$.

Tsvelik and Yevtushenko discovered the difference between two regimes that constitute different phases: Easy Axis (EA) with $J_z > J_\perp$ and Easy Plane (EP) with $J_z < J_\perp$. They found that in the EA-phase, all quasi particles are gapped and therefore, electric current cannot be supported by electrons. At $J_z = J_\perp$, $\mathbb{Z}_2$-(helical) symmetry is sponateously broken: In the EP-phase, only the bands of one helicity are gapped whereas the other branch remains gapless and allows quasiparticles of this helicty to travel along the lattice and to support the current (see Fig. 7).

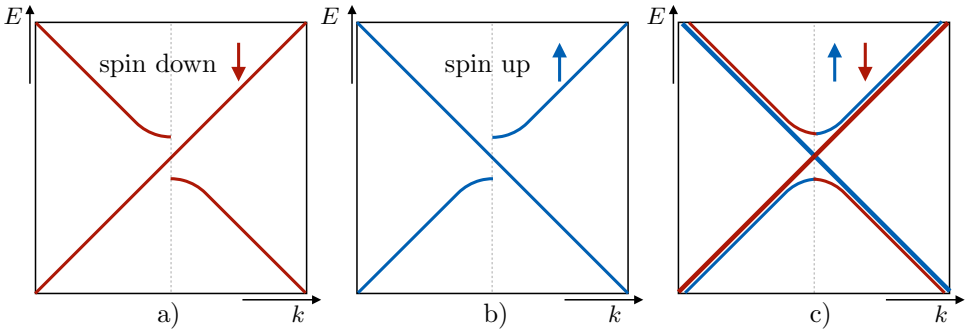

Fig. 7: Panels a) and b) show the dispersion relation for electrons in the two possible spin states in the Easy-Plane phase ($J_z < J_\perp$). In this phase, helicity is spontaniously broken and only electrons with a certain helicity (here $h = +1$) can propagate through the lattice whereas the band structure for the other helicity is gapped as shown in c).

Schimmel et al. showed in [19] that it is possible to define the vector product of two neighboring spins in the dense chain of magnetic moments as order parameter that dinstiguishes between the EP- and the EA-phase: $\mathcal{A}_c = \epsilon_{abc}\langle S^a(1)S^b(1+\xi_0)\rangle$. In the EP-phase, the spin components S^x and S^y are correlated which is graphically represented by a helix when the spin waves are plotted over position (see Fig. 8). The orientation of the helix is in one-to-one correspondance with helicity.

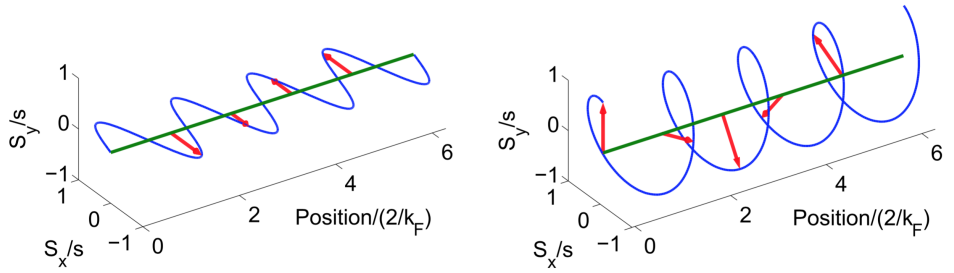

Fig. 8: A travelling spin wave in the EA (left) and EP (right) setup. Since S_x and S_y in the EA case are uncorrelated to leading order, only one contribution is shown. The orientation of the helix (right) corresponds to a well-defined helicity. For the other helcity, the orientation is inverted, adopted from [19].

The existence of robust helical modes is reminiscent of helical edge states in topological insulators though it should be emphasized that its origin lies in many body interaction effects whereas it is due to a topologically nontrivial bulk in topological insulators. Elastic single particle backscattering is surpressed because it would contain a spin flip which would violate the U(1) spin symmetry. In this sense, this helical state is symmetry protected.

1.2 Quantum Dots

In the main part of this thesis, the 1D helical wires that we discussed in the last section will play a central role. More precisely, we aim at describing the spin-to-charge conversion that we expect to take place when a 1D helical wire is tunnel coupled to a quantum dot (QD) that is out of equilibrium, i.e. has different and fixed probabilities of being occupied by ↑- and ↓-electrons (see Fig. 9). In the following, we will therefore shortly introduce quantum dots and describe the properties that are most important for our application. Furthermore, we will give an introduction to the tunneling Hamiltonian that will allow us to calculate the tunneling current between the 1D helical wire and the quantum dot that we will consider.

A quantum dot is defined as artificially produced nanostructure that is spatially strongly restricted, such that electrons that populate the quantum dot are quantized in energy. By definition it has the property that the time τ_{Thouless} that it takes the electron to cross the confining potential from one border to the other is much smaller than its lifetime τ_{life} and the dwelling time τ_{dwell} which is the time that the electron remains in the quantum dot:

$$\tau_{\text{Thouless}} \ll \tau_{\text{life}}, \tau_{\text{dwell}}. \tag{15}$$

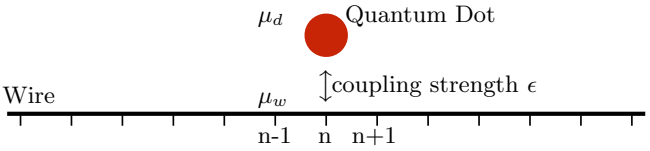

Fig. 9: Quantum dot coupled to a wire via tunneling with coupling strength ϵ and tunneling junction at site n. The quantum dot and the wire can have different chemical potentials μ_α. For our considerations, we replace the general wire by a helical wire.

This restriction implies that the electron's trajectory almost homogeneously covers the surface of the quantum dot (see Fig. 10). Therefore, no localization of an electron in the quantum dot is possible which justifies a zero-dimensional description of the QD.

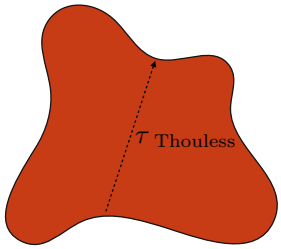

Fig. 10: By definition, the trajectory of an electron covers the confining potential almost homogeneously which corresponds to $\tau_{\text{Thouless}} \ll \tau_{\text{life}}, \tau_{\text{dwell}}$. This justifies a zero-dimensional description of the quantum dot.

As model, we consider a metallic island that is populated by electrons and carries its charge on the surface. With classical electrostatics, its potential energy due to its electric field is given by $E = Q^2/C$ where C denotes the capacitance. Since the charge Q consists of the charge contributions from single electrons, one can write $E = \frac{e^2}{C}N^2$ where N is the number of electrons in the QD. One can define the charging energy $E_C \equiv \frac{e^2}{C}$ which is the energy that is needed to add an electron to the neutral QD. To add the N's electron, it takes an electrostatic energy of $\Delta E = E_C(N^2 - (N-1)^2) = E_C(2N-1)$. Coming back to the energy scale, one defines for quantum dots that the energy spacing of different levels within the QD is not negligible with respect to the charging energy [12].

Since we want to investigate the electron exchange between a quantum dot and a 1D helical wire, we need to get an understanding of its transport properties that the next section will be dedicated to.

1.2.1 Transport properties

From a phenomenological point of view, it is natural to use a rate equation in order to describe the probability of the quantum dot to be in a certain state α. The rate of change from state α to state β is denoted: $\Gamma(\alpha \to \beta)$. In the stationary case, the change of the probability of finding the dot in state α, p_α is:

$$0 = \frac{\partial p_\alpha}{\partial t} = -p_\alpha \sum_\beta \Gamma(\alpha \to \beta) + \sum_\beta p_\beta \Gamma(\beta \to \alpha). \tag{16}$$

This equation is called *master equation*. The states α, β could be spin states, for example.

It is now possible to write the electric current in terms of the rates from the master equation:

$$I = \sum_{N,\alpha,\beta} p_{N,\alpha}(\Gamma(N, \alpha \to N+1, \beta) - (\Gamma(N, \alpha \to N-1, \beta)).$$

Due to energy conservation, the transitions that are described by the rates $\Gamma(\alpha \to \beta)$ can only take place if the change in energy,

$$\Delta E = (E(N \pm 1, \alpha) - E(N, \beta)) \pm (\mu_d - \mu_w),$$

is negative. The first term includes the internal energy difference in the dot, as well as the change in charging energy.

Since, for the transition of an electron in the wire with energy E_k to occur, there must be an electron in the wire at E_k and a hole in the dot that has the corresponding energy $E_k - \Delta E$, the transition rate Γ includes to the so-called Pauli factor, $f^{\mathrm{FD}}(E_k)\left(1 - f^{\mathrm{FD}}(E_k - \Delta E)\right)$:

$$\Gamma_{w\to d} = \frac{G}{e^2} \int dE_k \, f^{\mathrm{FD}}(E_k) \left[1 - f^{\mathrm{FD}}(E_k - \Delta E)\right] = \frac{G}{e^2} \frac{\Delta E}{e^{\beta \Delta E} - 1}. \tag{17}$$

The prefactor G is called *conductance* and is determined by the physical system. Taking tunneling into the opposite direction into account, one obtains analogously:

$$\Gamma_{d\to w} = \frac{G}{e^2} \int dE_k f^{\mathrm{FD}}(E_k - \Delta E)[1 - f^{\mathrm{FD}}(E_k)] = \frac{G}{e^2} \frac{\Delta E}{1 - e^{-\beta \Delta E}}. \tag{18}$$

Hence, the total tunneling current can be written:

$$I_T = e(\Gamma_{w\to d} - \Gamma_{d\to w}) = \frac{G}{e} \Delta E. \tag{19}$$

Consequently, if one knows the current, one can compute the conductance via the simple relation:

$$G = e \frac{I_T}{\Delta E}. \tag{20}$$

1.3 Tunneling Hamiltonian

In order to describe the electron exchange between the bulk of a system and a quantum dot via tunneling, one usually introduces a tunneling Hamiltonian which takes the following form (see Fig. 9):

$$\hat{H}_T = \epsilon(\hat{c}_n^\dagger \hat{d} + \hat{d}^\dagger \hat{c}_n). \tag{21}$$

where ϵ is the tunneling coupling strength. The continuous form of $\hat{H}_T$ for the tunnling between a quantum dot and a helical wire reads:

$$\hat{H}_T = \gamma \left(\hat{\Psi}^\dagger(x)\hat{d} + \hat{d}^\dagger \hat{\Psi}(x) \right) \big|_{x=0}. \tag{22}$$

with $\gamma := \frac{2\hbar v_F}{\sqrt{\lambda}} t$ where t is a dimensionless tunneling parameter and λ is a characteristic length for the contact that can be identified with the size of the quantum dot. In both expressions, the first term creates an electron in the wire at site n (or at position x) and annihilates one in the dot, the second one has the inverse effect. Performing the Fourier transform of Eq. (21) to momentum space and choosing the tunneling junction to be located at $n = 0$, one obtains:

$$\hat{H}_T = \epsilon \sum_k (\hat{c}_k^\dagger \hat{d} \ + \hat{d}^\dagger \hat{c}_k).$$

Consequently, the quantum dot couples to every momentum state in the wire. If ϵ is small, the effect of the tunneling Hamiltonian on the isolated systems of the wire and the quantum dot can be treated perturbatively.

1.4 Tunneling Conductance Between Metallic Contact and Chiral Wire

In the main part of this thesis, we compute the tunneling conductance between a helical wire and a quantum dot. Among other analytic methods, we explicitly solve the Schrödinger equation which allows us to find an expression for the conductance. Out method is similar to that of Fillippone and Brouwer in [5], where tunneling between two quantum wires is considered. We will briefly explain the method in this section.

Fillippone an Brouwer considered a spinless one-dimensional wire that is tunnel coupled to a metallic contact which can be the tip of a scanning probe or an integer quantum Hall edge state (see Fig. 11). The electrons in the wire are considered to be spinless and to have only one chiral mode which means that they can only travel in one direction. Interactions between electrons are neglected. The Hamiltonian describing this system reads:

$$\hat{H} = \hat{H}_C + \hat{H}_W + \hat{H}_T, \qquad (23)$$

where

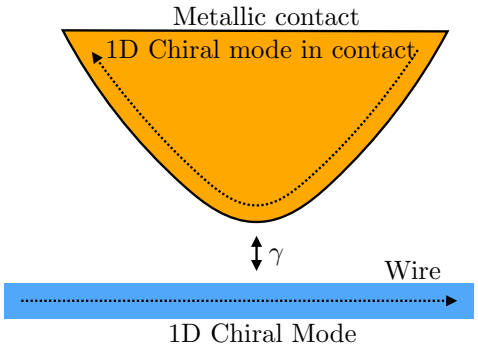

Fig. 11: Tunneling contact between a metallic contact and a one-dimensional wire which is taken to have only a single chiral state, adapted from [5].

$$\hat{H}_C = r \int_{-\infty}^{\infty} dx \hat{c}^\dagger(x)(-i\hbar u_\mathrm{F}\partial_x)\hat{c}(x) \qquad (24)$$

$$\hat{H}_W = \int_{-\infty}^{\infty} dx \hat{\Psi}^\dagger(x)(-i\hbar v_\mathrm{F}\partial_x)\hat{\Psi}(x) \qquad (25)$$

$$\hat{H}_T = \gamma\hat{\Psi}^\dagger(0)\hat{c}(0) + \gamma^*\hat{c}^\dagger(0)\hat{\Psi}(0). \qquad (26)$$

Here, the operators $\hat{c}$ and $\hat{\Psi}$ describe electrons in the contact and in the wire, respectively. The prefactor $r = \pm$ in Eq. (24) determines the direction of motion of the chiral electrons in the contact with respect to the wire. The velocites u_F and v_F denote the Fermi velocity in the contact and in the wire, respectively.

1.4.1 Regularization

In the following, a regularization function is introduced in order to define the tunneling Hamiltonian that reflects the tunnel junction at $x = 0$. The reason why is

it needed is related to the fact that we deal with 1D Dirac-Fermions whose characteristic property is a linear dispersion relation. We will briefly explain why this requires a regularizaion function:
Assuming particles with a quadratic dispersion relation, when solving the Schrödinger equation for a delta-potential $V = \alpha\delta(x)$,

$$\left(-\frac{\hbar^2}{2m}\frac{d^2}{dx^2} + \alpha\delta(x)\right)\Psi(x) = \epsilon\Psi(x), \tag{27}$$

one needs to integrate over a small strip $-\epsilon < x < \epsilon$ [6]. In the next step, one sets $\epsilon \to 0$. This yields:

$$\xrightarrow{\lim_{\epsilon\to 0}\int_{-\epsilon}^{\epsilon} dx} \lim_{\epsilon\to 0} -\frac{\hbar^2}{2m}(\Psi'(\epsilon) - \Psi'(-\epsilon)) + \alpha\Psi(0) = 0 \tag{28}$$

$$\leftrightarrow \Psi'(0^+) - \Psi'(0^-) = \frac{\alpha 2m}{\hbar^2}\Psi(0). \tag{29}$$

The right hand side in Eq. (28) is zero because it is the area of a sliver with vanishing width and finite height. One must impose the boundary condition that the wavefunction be continuous at $x = 0$. The logarithmic derivative of the wavefunction at this point, $\frac{\Psi'(0)}{\Psi(0)} = (\log\Psi(x))'|_{x=0}$, turns out to be discontinuous.

Contrarily, the case of a linear dispersion relation leads to an unphysical discontinuity in the wavefunction itself:

$$\left(i\hbar v_{\mathrm{F}}\frac{d}{dx} + \alpha\delta(x)\right)\Psi(x) = \epsilon\Psi(x) \tag{30}$$

$$\xrightarrow{\int_{-\epsilon}^{\epsilon} dx} i\hbar v_{\mathrm{F}}(\Psi(\epsilon) - \Psi(-\epsilon)) + \alpha\Psi(0) = 0 \tag{31}$$

$$\leftrightarrow (\Psi(\epsilon) - \Psi(-\epsilon)) = i\frac{\alpha}{\hbar v_{\mathrm{F}}}\Psi(0). \tag{32}$$

This contradicts the physical necessity of continuity of the wavefunction. The problem can be solved by introducing a so-called regularization function $f(x)$ which has the effect of opening an interval in which the potential is applied.

Fillippone and Brouwer defined the following regularization function $f(x)$:

$$f(x) = \frac{1}{2\delta}\Theta(\delta - |x|), \tag{33}$$

where δ is the regularization scale and $\Theta(x)$ is the Heavyside step function. Using this regularization function, they suggested two different regularizations:

Choice I) $\hat{\Psi}(0) \to \int dx f(x)\hat{\Psi}(x)$ and $\hat{c}(0) \to \int dx f(x)\hat{c}(x)$

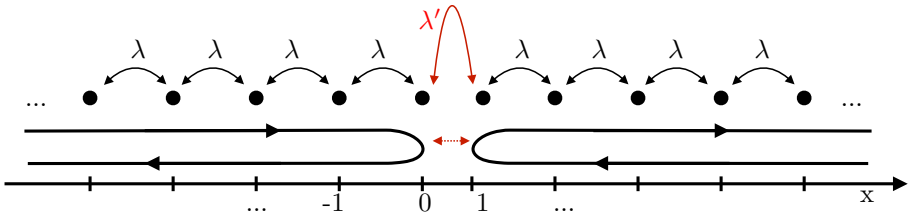

Fig. 12: Spinless fermions on two semi-infinite lattices hopping on nearest neighbor sites with amplitude λ. The electrons can jump from one lattice to the other with hopping amplitude $\lambda' \neq \lambda$. The indicated paths can be continously transformed to chiral modes in the contact and the wire, respectively, adapted from [5].

Choice II) $\hat{\Psi}^\dagger(0)\hat{c}(0) \to \int dx f(x)\hat{\Psi}^\dagger(x)\hat{c}(x)$.

To leading (second) order, the expressions for the conductance coincide in all three cases:

$$G = \frac{4e^2t^2}{h} + \mathcal{O}(t^4), \tag{34}$$

where $t = \frac{\gamma}{2\hbar\sqrt{v_F u_F}}$ is a dimensionless tunneling parameter. However, the different regularization choices turn out to lead to different results in the conductance for large tunneling. An exemplary derivation for case (I) is given in Appendix A.

It is useful to take a closer look at the physical interpretation of the individual regularization choices:

Choice I) The conductance in this case reads $G = \frac{4e^2t^2}{h(1+t^2)^2}$. The physical situation is analogous to two semi-infinite fermionic lattices whose lattice sites are connected by a hopping amplitude λ. The hopping amplitude between the two semi-infinite chains is $\lambda' \neq \lambda$ (see Fig. 12). An electron at site $x = 0$ can therefore either be reflected or transmitted onto the other lattice. The resulting paths are indicated in Fig. 12. It is possible to continuously transform them into chiral modes which can be identified with the wire and the contact. A reflection at $x = 0$ in this model is therefore not in contradiction to the chirality in the wires since it simply corresponds to an electron crossing the tunneling section without tunneling to the other wire (see Fig. 11). A transmission in Fig. 12, on the other hand, corresponds to a tunneling event in the setup from Fig. 11. The fermionic-chain model is described by the Schrödinger equation:

$$E\Psi_j = -\lambda[\Psi_{j+1}(1-\delta_{0j}) + \Psi_{j-1}(1-\delta_{1j})] - \lambda'[\Psi_1\delta_{0j} + \Psi_0\delta_{1j}]. \tag{35}$$

A scattering approach with eigenvectors of the form $\Psi_j \propto e^{ik_F j} + \rho e^{-ik_F j}$ for $j < 0$ and $\Psi_j \propto \tau e^{ik_F j}$ for $j > 0$ leads to a transmission amplitude of

$$\tau = \frac{2(\lambda'/\lambda)}{1 + (\lambda'/\lambda)^2}. \tag{36}$$

Making the identification $\frac{\lambda'}{\lambda} = t$, this can be seen to be equivalent to the result that we derived in Appendix A:

$$G = \frac{e^2}{h}|\tau|^2 = \frac{e^2}{h}\frac{4(\lambda'/\lambda)^2}{(1 + (\lambda'/\lambda)^2)^2} \xrightarrow{\frac{\lambda'}{\lambda}=t} \frac{4e^2t^2}{h(1+t^2)^2}. \tag{37}$$

Choice II) This regularization choice is sensitive to the respective chirality of the contact and the wire. For opposite chiralities, one obtains a conductance of $G = \frac{e^2}{h}\tanh^2(2t)$. In the limit $t \to \infty$, H_T opens up a gap in the contact and the wire which leads to complete backscattering that corresponds to full transmission into the other wire. This regularization choice is analogous to the opening of a quantum point contact between two quantum Hall edge states with opposite chiralities.
For equal chiralities, however, electrons oscillate coherently between the contact and the wire and the transmission strongly depends on the strength of the contact.
The conductance in this case reads:

$$G = \frac{e^2}{h}\sin^2(2t). \tag{38}$$

2 Statement of the Problem and Outline of the Thesis

The goal of this thesis is to describe the spin-to-charge conversion that we expect to take place when a quantum dot that is out of equilibrium (different occupation probabilities for $\uparrow$- and $\downarrow$-electrons are fixed by a bath) is tunnel coupled to a helical wire.
We aim at understanding the limitations of phenomenological rate equations and the necessity of regularization in the tunneling Hamiltonian. Furthermore, we want to find a general expression for the spin-to-charge conversion which is valid for different realizations of the quantum dot. Our next goal is then to make connections between different models and to relate them to different standard-way approaches, such as the scattering approach and a perturbative approach.

For these purposes, we consider different analytic techniques that we eventually compare. After introducing the setup that we base our considerations upon, we proceed as follows:

1. We use phenomenological rates from the master equation to extract an expression for the induced current in the helical wire.

2. We compute the spin-dependent tunneling current between the quantum dot and the helical wire by explicitly solving the Schrödinger equation. This will allow us to find an expression for the induced current in the helical wire.

3. We make a perturbative approach and compute the induced current in second order of tunneling. This allows us to implement different models for the quantum dot which we can relate to the result that we obtained from the Schrödinger equation and the one that we found in the phenomenological approach. Subsequently, we verify our results by comparing them to the result that we obtain from Fermi's Golden rule.

4. The result is put into perspective with the case of tunneling between two 1D chiral states as investigated by Fillippone and Brouwer in Ref. [5] (see Sec. 1.4). The physical differences between our setup and theirs are discussed.

3 Main part

3.1 Tunneling (spin-)current between a magnetized Quantum Dot and a helical wire via the master equation

Before performing the steps outlined above, we will briefly introduce the setting that we base our considerations upon. The initial setup is the following: Two parallel helical wires are tunnel coupled to a quantum dot that is situated in between the two wires (see Fig. 13).

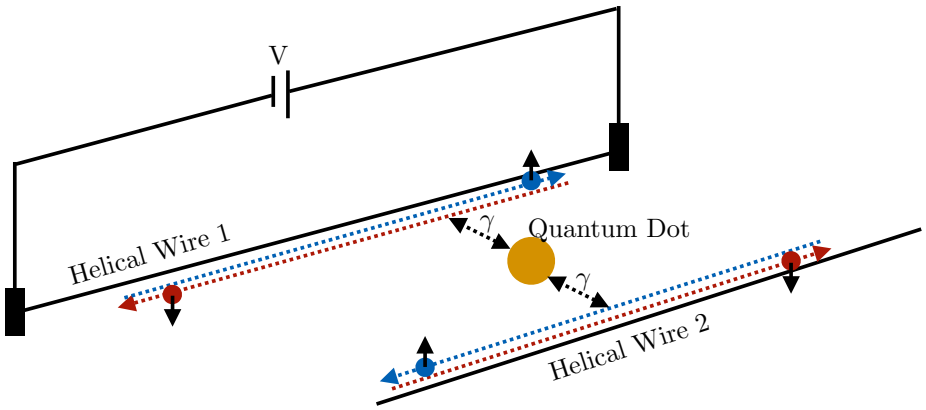

Fig. 13: Setup: A quantum dot is tunnel coupled to two helical wires. Applying a voltage in one helical wire 1 leads to the suppression of one of the two spin-currents which results in a net magnetization of the quantum dot.

This setup has been studied in terms of master equations in Ref. [15]. They assumed strong Coulomb repulsion which motivates the limitation of the quantum dot population to a single electron. The change of the probabilities for the quantum dot to be either empty or occupied by an electron of either spin state is:

$$\partial_t p_\uparrow = (\Gamma_{\text{in},1} + \Gamma_{\text{in},2})p_0 - (\Gamma_{\text{out},1} + \Gamma_{\text{out},2})p_\uparrow + \Gamma_S(p_\downarrow - p_\uparrow) \tag{39}$$

$$\partial_t p_\downarrow = (\Gamma_{\text{in},1} + \Gamma_{\text{in},2})p_0 - (\Gamma_{\text{out},1} + \Gamma_{\text{out},2})p_\downarrow + \Gamma_S(p_\uparrow - p_\downarrow) \tag{40}$$

$$\partial_t p_0 = (\Gamma_{\text{out},1} + \Gamma_{\text{out},2})(p_\uparrow + p_\downarrow) - 2(\Gamma_{\text{in},1} + \Gamma_{\text{in},2})p_0 \tag{41}$$

The rates $\Gamma_{\text{in(out)},i}$ reflect tunneling rates into (out of) the quantum dot from (into) wire i. Γ_S is the spin-flip rate within the quantum dot.
By applying a voltage in wire 1, one can prohibit electrons in state $\sigma =\uparrow$ to travel in wire 1 ($\Gamma_{\text{in},1} = \Gamma_{\text{out},1} = 0$ for spin $\uparrow$-electrons). Assuming the stationary case (all

of the above time derivatives are set to zero), one obtains [15]:

$$p_\uparrow = \frac{\Gamma_{\text{in},2}}{\Gamma_{\text{in},1} + 2\Gamma_{\text{in},2} + \frac{1}{2}\Gamma_{\text{out},1} + \Gamma_{\text{out},2}} \tag{42}$$

$$p_\downarrow = \frac{\Gamma_{\text{in},1} + \Gamma_{\text{in},2}}{\Gamma_{\text{in},1} + 2\Gamma_{\text{in},2} + \frac{1}{2}\Gamma_{\text{out},1} + \Gamma_{\text{out},2}} \tag{43}$$

$$p_0 = \frac{\frac{1}{2}\Gamma_{\text{out},1} + \Gamma_{\text{out},2}}{\Gamma_{\text{in},1} + 2\Gamma_{\text{in},2} + \frac{1}{2}\Gamma_{\text{out},1} + \Gamma_{\text{out},2}} \tag{44}$$

If all rates are set to an equal value, one obtains for the magnetization probabilities:

$$p_0 = \frac{1}{3} \text{ and } p_\uparrow = \frac{2}{9} \text{ and } p_\downarrow = \frac{4}{9}, \tag{45}$$

which shows a magnetization of the quantum dot. The exact values for the probabilities are not important in our case; we simply note that they differ for the two spin states.
This can be reflected by different chemical potentials for the two spin-sates in the quantum dot (see Fig. 14).

Fig. 14: A net magnetization gives rise to spin-dependent chemical potentials in the quantum dot.

A zero-net-magnetization would correspond to $\mu_\uparrow = \mu_\downarrow$. In our calculations, we will simply assume a magnetized quantum dot with fixed $p_\uparrow, p_\downarrow$ that we can interpret as a source that injects electrons in the helical wire 2.

The rates yield an expression for the tunneling current. The outgoing flow of charge for spin state σ must be proportional to the probability of an electron being in the QD, p_σ, and the outgoing tunnel rate Γ_{out}. The incoming current must be proportional to the probability of the quantum dot being empty p_0, and the incoming rate Γ_{in}. Hence, the total tunneling current for spin state σ can be written as:

$$I_T^\sigma = (\Gamma_{\text{out}}\, p_\sigma - \Gamma_{\text{in}}\, p_0)\, e. \tag{46}$$

3.1.1 Induced current in the helical wire

Assuming that electrons with spin $\sigma =\downarrow$ travel to the right in the helical wire, one can make the following considerations: In the part of the wire left to the tunneling junction which we take to be located at $x = 0$, the current for $\sigma =\downarrow$ is the one of the unperturbed helical wire since electrons cannot backscatter at the junction:

$$I^{\downarrow}_{x<0} = I^{\downarrow}_{equ}. \tag{47}$$

Therefore, the effect of the quantum dot for this spin state can only be observed in the right side of the wire. The current in the right side is the sum of the equilibrium current in the left side and the tunneling current which can be positive or negative:

$$I^{\downarrow}_{x>0} = I^{\downarrow}_{equ} + I^{\downarrow}_{T} \tag{48}$$

The other spin-state is analogous. The total electric current in the wire is:

$$\text{left side: } I_{x<0} = I^{\downarrow}_{equ} + I^{\uparrow}_{equ} + I^{\uparrow}_{T} \tag{49}$$

$$\text{right side: } I_{x>0} = I^{\uparrow}_{equ} + I^{\downarrow}_{equ} + I^{\downarrow}_{T}. \tag{50}$$

As demonstrated in Appendix D, the effective electric current in an unperturbed helical wire is zero, $I^{\downarrow}_{equ} + I^{\uparrow}_{equ} = 0$. Consequently, Eqs. (49) and (50) simplify to:

$$\text{left side: } I_{x<0} = I^{\uparrow}_{T} \tag{51}$$

$$\text{right side: } I_{x>0} = I^{\downarrow}_{T}. \tag{52}$$

Hence, due to the different direction of motion for the different spin states, the effective induced current is:

$$I_{\text{ind}} = I^{\uparrow}_{T} - I^{\downarrow}_{T}. \tag{53}$$

This equation is general and independent of the approach that one chooses in order to compute the spin-dependent tunneling current.

In the case of phenomenological rate equations one finds that, if the rates are taken to be spin-independent, the induced current in the helical wire becomes:

$$I_{\text{ind}} = I^{\uparrow}_{T} - I^{\downarrow}_{T} \tag{54}$$

$$= (\Gamma_{\text{out}}\, p_{\uparrow} - \Gamma_{\text{in}}\, p_0)\, e - (\Gamma_{\text{out}}\, p_{\downarrow} - \Gamma_{\text{in}}\, p_0)\, e \tag{55}$$

$$= e\Gamma_{\text{out}}\, (p_{\uparrow} - p_{\downarrow}). \tag{56}$$

One can deduce that if the quantum dot is magnetized, an electric current is induced in the helical which illustrates the spin-to-charge-conversion that we are able to observe in our system.

3.2 Tunneling Conductance via the Schrödinger equation

The approach with the master equation confirms the intuition that the non-equilibrium quantum dot induces an electric current in the helical wire but it fails to provide an explicit expression for the current. Moreover, this approach cannot take regularization into account which we showed to be necessary for 1D Dirac Fermions (see Sec. 1.4.1). In order to include regularization, we choose a scattering approach. The goal of this section is to compute the tunneling conductance by explicitly solving the Schrödinger equation in the setup of a helical wire that is coupled to a magnetized quantum dot that is out of equilibrium. The Hamiltonians have the following form:

$$\hat{H}_T = \sum_\sigma \gamma \hat{\Psi}^\dagger_\sigma(0)\hat{d}_\sigma + \gamma \hat{d}^\dagger_\sigma \hat{\Psi}_\sigma(0) \tag{57}$$

$$\hat{H}_D = \sum_\sigma \epsilon_{d_\sigma} \hat{d}^\dagger_\sigma \hat{d}_\sigma \tag{58}$$

$$\hat{H}_W = \sum_\sigma \int dx \hat{\Psi}^\dagger_\sigma(x)(s_\sigma i\hbar v_\mathrm{F}\partial_x)\hat{\Psi}_\sigma(x) \tag{59}$$

with

$$s_\sigma = \begin{cases} - & \text{for } \sigma = \uparrow \\ + & \text{for } \sigma = \downarrow \end{cases}.$$

$\hat{H}_T$ is the tunneling Hamiltonian that describes the tunneling junction at $x = 0$ for which we will further introduce a regularization, $\hat{H}_D$ and $\hat{H}_W$ are the Hamiltonians for the quantum dot and the wire for the uncoupled system. $\hat{d}_\sigma$ and $\hat{\Psi}_\sigma$ describe electrons in the quantum dot and in the wire, respectively; ϵ_{d_σ} is the spin dependent energy in the dot that we define as:

$$\epsilon_{d_\sigma} \coloneqq \epsilon_d + \mu_\sigma, \tag{60}$$

where μ_σ is the shift in the chemical potential in the QD for electrons in spin state σ.

Moreover, we define

$$\gamma \coloneqq \frac{2\hbar v_\mathrm{F}}{\sqrt{\lambda}} t, \tag{61}$$

where λ is a characteristic length of the tunnel junction that we define to be the size of the quantum dot, t is a dimensionless tunneling parameter that determines the tunneling strength and v_F denotes the Fermi velocity in the wire. For the reasons explained above, a regularization function is introduced which we define as follows:

$$f(x) = \Theta(\delta - |x|)/(2\delta),$$

such that $\Psi(x=0) \coloneqq \int dx \Psi(x) f(x)$. Physically, this reflects an interval of size 2δ in the wire in which electrons can tunnel to or from the QD (see Fig. 15). Since the QD is assumed to be zero-dimensional, such a regularization is not necessary for the dot and one is therefore not left with many alternatives for boxlike regularization schemes.

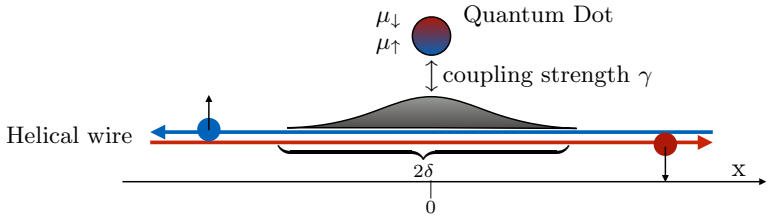

Fig. 15: Regularization function: In an interval of size 2δ, electrons can tunnel from the helical wire to the quantum dot and vice versa.

The zero in energy can be tuned such that the Schrödinger equation in the interval $-\delta < x < \delta$ reads:

$$E_\sigma d_\sigma = \epsilon_{d_\sigma} d_\sigma + \frac{\gamma}{2\delta} \int_{-\delta}^{\delta} dx \Psi_\sigma(x) \tag{62}$$

$$0 = (s_\sigma i\hbar v_\mathrm{F} \partial_x) \Psi_\sigma(x) + \frac{\gamma}{2\delta} d_\sigma \tag{63}$$

Here,

$$E_\sigma = E_{d_\sigma} - E_{w_\sigma} \tag{64}$$

where E_{d_σ} and E_{w_σ} are the energy eigenvalues of the quantum dot and of the wire, respectively.
This set of equations can be solved for each spin state independently since they are not coupled and global spin is conserved. For $\sigma = \uparrow$:

$$E_\uparrow d_\uparrow = \epsilon_{d_\uparrow} d_\uparrow + \frac{\gamma}{2\delta} \int_{-\delta}^{\delta} dx \Psi_\uparrow(x) \tag{65}$$

$$0 = (-i\hbar v_\mathrm{F} \partial_x) \Psi_\uparrow(x) + \frac{\gamma}{2\delta} d_\uparrow \tag{66}$$

Following Ref. [5], let us make a linear ansatz for the wire. Due to the fact that the QD is zero-dimensional, its wavefunction must be constant. This corresponds to the situation where only its zero-momentum mode is kept:

$$\begin{aligned} \Psi_\uparrow &= Ax + B \\ d_\uparrow &= C = const. \end{aligned} \tag{67}$$

Inserting this into Eqs. (65) and (66):

$$0 = (\epsilon_{d_\uparrow} - E_\uparrow)d_\uparrow + \frac{\gamma}{2\delta}2B\delta \tag{68}$$
$$0 = -i\hbar v_\mathrm{F} A + \frac{\gamma}{2\delta}d_\uparrow$$

We can deduce $\Psi_\uparrow(x)$ in dependence of $d_\uparrow$:

$$\Psi_\uparrow(x) = -\frac{i\gamma d_\uparrow}{2\delta\hbar v_\mathrm{F}}x - \frac{(\epsilon_{d_\uparrow} - E_\uparrow)d_\uparrow}{\gamma} = \left(-\frac{i\gamma}{2\delta\hbar v_\mathrm{F}}x - \frac{(\epsilon_{d_\uparrow} - E_\uparrow)}{\gamma}\right)d_\uparrow. \tag{69}$$

As defined in Eq. (61), we insert the dimensionless tunneling parameter $t = \frac{\gamma\sqrt{\lambda}}{2\hbar v_\mathrm{F}}$ where λ denotes a characteristic length of the junction that can be identified with the size of the quantum dot:

$$\Psi_\uparrow(x) = \left(-\frac{it}{\delta\sqrt{\lambda}}x - \frac{(\epsilon_{d_\uparrow} - E_\uparrow)\sqrt{\lambda}}{2\hbar v_\mathrm{F} t}\right)d_\uparrow. \tag{70}$$

It is only possible to choose a single boundary condition since we are dealing with a set of two equations with three parameters A, B and C. Thus, adding one boundary conditions fixes all three parameters. We choose the constant wavefunction in the quantum dot to be:

$$d_\uparrow = \sqrt{\frac{\lambda}{2\pi\hbar v_\mathrm{F}}}. \tag{71}$$

Thus, the wavefunction in the wire, $\Psi(x)$, will be normalized with dimensions that correspond to the square root of its density of states (DoS):

$$\rho_w = \frac{1}{2\pi}\frac{\partial k}{\partial \epsilon_k} = \frac{1}{2\pi\hbar v_\mathrm{F}}. \tag{72}$$

Since the change of the amplitude that the wavefunction $\Psi(x)$ acquires along the tunneling section reflects the probability of an electron to tunnel from/to the wire and since $\Psi(x)$ is linear in the interval $-\delta < x < \delta$, we can identify the transmission probability between the quantum dot and an electron in the wire as:

$$T_\uparrow(\epsilon) = \left|\frac{\Psi_\uparrow(\delta) - \Psi_\uparrow(-\delta)}{d_\uparrow}\right|^2 \cdot \frac{\mathcal{A}(\epsilon)}{\rho_w} \tag{73}$$
$$= \frac{4t^2}{\lambda}\frac{\mathcal{A}(\epsilon)}{\rho_w}, \tag{74}$$

where we have introduced the spectral density of states in the quantum dot,

$$\mathcal{A}(\epsilon) = \frac{1}{\pi}\frac{\gamma^2\rho_w}{(\epsilon - \epsilon_d)^2 + (\gamma^2\rho_w)^2} \overset{\gamma = t\frac{2\hbar v_\mathrm{F}}{\sqrt{\lambda}}}{=} \frac{1}{\pi}\frac{\frac{t^2}{\rho_w\pi^2\lambda}}{(\epsilon - \epsilon_d)^2 + (\frac{t^2}{\rho_w\pi^2\lambda})^2} \tag{75}$$

that we derived explicitly in App. B. Knowing the energy-dependent transmission value and comparing to Eqs. (17) and (18), one can write the total tunneling current for this spin state:

$$I_T^{\uparrow} = \frac{e}{h} \int d\epsilon_k \, T_{\uparrow}(\epsilon_k) \, \left(f_{\mathrm{QD}}(\epsilon_k) - f_{\mathrm{W}}(\epsilon_k) \right). \tag{76}$$

The form of the transmission value is a non-trivial function of the tunneling parameter t. In the limit $t \to \infty$, it becomes constant:

$$T_{\uparrow} \xrightarrow{t \to \infty} 4\pi = const. \tag{77}$$

In the considerations by Fillippone and Brouwer that we introduced above, however, it was shown that only for small tunneling, the expression for the transmission value is unambiguous in order t^2, i.e. independent of the regularization choice. $\mathcal{A}(\epsilon)$ has the shape of a Lorentzian peak. Consequently, for small t, it becomes:

$$\mathcal{A}(\epsilon) = \frac{1}{\pi} \frac{\frac{t^2}{\rho_w \pi^2 \lambda}}{(\epsilon - \epsilon_d)^2 + (\frac{t^2}{\rho_w \pi^2 \lambda})^2} \xrightarrow{t \ll 1} \delta(\epsilon - \epsilon_d). \tag{78}$$

This substantially simplifies the integral in Eq. (76) which becomes:

$$I_T^{\uparrow} = \frac{e}{h} \int d\epsilon_k \, 4 \frac{2\pi\hbar v_{\mathrm{F}} t^2}{\lambda} \delta(\epsilon_k - \epsilon_d) \left(f(\epsilon_k + \mu_{\uparrow}) - f(\epsilon_k) \right) \tag{79}$$

$$= 4 \frac{e}{h} \frac{t^2 2\pi\hbar v_{\mathrm{F}}}{\lambda} \left(f(\epsilon_d + \mu_{\uparrow}) - f(\epsilon_d) \right). \tag{80}$$

Hence, for small $\mu_{\uparrow}$, such that a linear response approximation is valid, the conductance is:

$$G_{\uparrow} = e \frac{I_T^{\uparrow}}{\mu_{\uparrow}} = 4 \frac{e^2}{h \mu_{\uparrow}} \frac{t^2 2\pi\hbar v_{\mathrm{F}}}{\lambda} \left(f(\epsilon_d + \mu_{\uparrow}) - f(\epsilon_d) \right). \tag{81}$$

The calculation for the other spin state, $\sigma = \downarrow$, is analogous though it should be emphasized that the chemical potentials differ in their value.

Besides the trivial temperature-dependence of the Fermi-Dirac-distributions, this result is temperature-independent. According to Eq. (53), the induced current in the helical wire becomes:

$$I_{\mathrm{ind}} = I_T^{\uparrow} - I_T^{\downarrow} \tag{82}$$

$$= 4 \frac{et^2}{h} \frac{2\pi\hbar v_{\mathrm{F}}}{\lambda} \big(f(\epsilon_d + \mu_{\uparrow}) - f(\epsilon_d) - f(\epsilon_d + \mu_{\downarrow}) + f(\epsilon_d) \big) \tag{83}$$

$$= 4 \frac{et^2}{h} \frac{2\pi\hbar v_{\mathrm{F}}}{\lambda} \left(f(\epsilon_d + \mu_{\uparrow}) - f(\epsilon_d + \mu_{\downarrow}) \right). \tag{84}$$

From this expression it becomes clear that, for different chemical potentials $\mu_\uparrow$ and $\mu_\downarrow$ (which corresponds to a magnetization of the quantum dot), there will be an effective electric current in the helical wire. We refer to this process as spin-to-charge-conversion.

3.3 Perturbative Calculation of the Tunneling Current

The goal of this section is to calculate the perturbative tunneling current using methods of quantum statistics. This will allow us to find a generic expression for the induced current in different models for the quantum dot that we can easily implement in the calculation. The difference in Fermi-Dirac distributions in Eq. (76) corresponds to a specific model, namely one where the quantum dot has two uncorrelated states for electrons with spin $\uparrow$ and $\downarrow$ and energy ϵ_d. This section helps to understand what changes if we modify the model by limiting the quantum dot to a single electron as done in Ref. [15] (see Sec. 3.1).

3.3.1 Induced Current via Trotter formula

In this subsection, we want to apply the Trotter Formula to obtain an expression for the induced current. The following ansatz reflects a situation in equilibrium and we expect therefore to find a zero-current. However, it yields a useful form for this zero-current which enables us to make a little manipulation by hand in order to impose the non-equilibrium-situation.

First, the Hamiltonian is split into $\hat{H}_0$ for the helical wire and the quantum dot without tunneling, and $\hat{H}_1$ as tunneling Hamiltonian:

$$\hat{H}_0 = \hbar v_\mathrm{F} \sum_k k(\hat{c}^\dagger_{k,\uparrow}\hat{c}_{k,\uparrow} - \hat{c}^\dagger_{k,\downarrow}\hat{c}_{k,\downarrow}) + \sum_\sigma \epsilon_{d,\sigma}\hat{d}^\dagger_\sigma\hat{d}_\sigma \tag{85}$$

$$\hat{H}_1 = \gamma \sum_\sigma (\hat{\Psi}^\dagger_\sigma(x)\hat{d}_\sigma + \hat{d}^\dagger_\sigma\hat{\Psi}_\sigma(x))\big|_{x=0}. \tag{86}$$

Defining the current operator $\hat{I}_\mathrm{ind} = \frac{ie}{\hbar}\gamma\sum_{k,\sigma} s_\sigma(\hat{\Psi}^\dagger_{k,\sigma}\hat{d}_\sigma - \hat{d}^\dagger_\sigma\hat{\Psi}_{k,\sigma})$, where $s_\uparrow = +$ and $s_\downarrow = -1$. The average current can be written as:

$$\langle I_\mathrm{ind}\rangle^\mathrm{eq} = \frac{1}{Z}\langle \hat{I}_\mathrm{ind} e^{-\beta\hat{H}}\rangle \tag{87}$$

$$= \left(\underbrace{\frac{1}{Z}\sum_\alpha \langle \alpha,\uparrow | \hat{I}_\mathrm{ind} e^{-\beta(\hat{H}_0+\hat{H}_1)} |\alpha,\uparrow\rangle}_{(*)} + \frac{1}{Z}\sum_\alpha \langle \alpha,\downarrow | \hat{I}_\mathrm{ind} e^{-\beta(\hat{H}_0+\hat{H}_1)} |\alpha,\downarrow\rangle \right) \tag{88}$$

Z denotes the partition function that we will turn to, later. For the sake of clarity, we will focus on the expression in in the underbrace (*) since the second term in the brace can be treated analogously. After having evaluated (*), we will return to

Eq. (88) to obtain the result. The Trotter formula yields (see App. C):

$$(*) = -\frac{\beta}{Z} \lim_{n\to\infty} \sum_{m=1}^{n} \sum_{\alpha} \langle\alpha|\hat{I}_{\text{ind}} e^{-\beta\hat{H}_0 \frac{m}{n}} \frac{\hat{H}_1}{n} e^{-\beta\hat{H}_0 \frac{n-m}{n}} |\alpha\rangle \tag{89}$$

Since the spin states do not mix and global spin is conserved, this expression can be evaluated for each spin state separately. For simplicity, the σ's are dropped in the notation for the calculation that is valid for either one of the spin states.

We insert unity $\mathbb{1} = \sum_i |i\rangle\langle i|$ between the single operators where the states $|i\rangle = |\delta\rangle, |\lambda\rangle, |\gamma\rangle$ denote eigenstates of $\hat{H}_0$.
Eq. (88) becomes:

$$(*) = -\frac{\beta}{Z} \lim_{n\to\infty} \sum_{m=1}^{n} \sum_{\alpha,\delta\lambda,\gamma} \langle\alpha|\hat{I}_{\text{ind}}|\delta\rangle\langle\delta|e^{-\beta\hat{H}_0 \frac{m}{n}}|\lambda\rangle\langle\lambda|\frac{\hat{H}_1}{n}|\gamma\rangle\langle\gamma|e^{-\beta\hat{H}_0 \frac{n-m}{n}}|\alpha\rangle \tag{90}$$

$$= -\frac{\beta}{Z} \lim_{n\to\infty} \sum_{m=1}^{n} \sum_{\alpha,\delta,\lambda,\gamma} \langle\alpha|\hat{I}_{\text{ind}}|\delta\rangle\langle\lambda|\frac{\hat{H}_1}{n}|\gamma\rangle \underbrace{\langle\delta|e^{-\beta\hat{H}_0 \frac{m}{n}}|\lambda\rangle}_{\langle\delta|e^{-\beta\hat{H}_0 \frac{m}{n}}|\delta\rangle\delta_{\delta,\lambda}} \underbrace{\langle\gamma|e^{-\beta\hat{H}_0 \frac{n-m}{n}}|\alpha\rangle}_{\langle\alpha|e^{-\beta\hat{H}_0 \frac{n-m}{n}}|\alpha\rangle\delta_{\alpha,\gamma}} \tag{91}$$

$$= -\frac{\beta}{Z} \lim_{n\to\infty} \sum_{m=1}^{n} \sum_{\alpha,\delta} \langle\alpha|\hat{I}_{\text{ind}}|\delta\rangle\langle\delta|\frac{\hat{H}_1}{n}|\alpha\rangle\langle\delta|e^{-\beta\hat{H}_0 \frac{m}{n}}|\delta\rangle\langle\alpha|e^{-\beta\hat{H}_0 \frac{n-m}{n}}|\alpha\rangle. \tag{92}$$

The terms containing m or n can be rewritten:

$$\lim_{n\to\infty} \sum_{m=1}^{n} \frac{1}{n} \langle\delta|e^{-\beta\hat{H}_0 \frac{m}{n}}|\delta\rangle\langle\alpha|e^{-\beta\hat{H}_0 \frac{n-m}{n}}|\alpha\rangle = \lim_{n\to\infty} \sum_{m=1}^{n} \frac{1}{n} e^{-\beta\epsilon_\delta \frac{m}{n}} e^{-\beta\epsilon_\alpha \frac{n-m}{n}} \tag{93}$$

$$= \lim_{n\to\infty} \sum_{m=1}^{n} \frac{1}{n} e^{-\beta(\epsilon_\delta-\epsilon_\alpha)\frac{m}{n}} e^{-\beta\epsilon_\alpha} = \lim_{n\to\infty} \sum_{m=0}^{n} \frac{1}{n} e^{-\beta(\epsilon_\delta-\epsilon_\alpha)\frac{m}{n}} e^{-\beta\epsilon_\alpha} - \underbrace{\lim_{n\to\infty} \frac{e^{-\beta\epsilon_\alpha}}{n}}_{=0}. \tag{94}$$

Because $\hat{H}_1$ and $\hat{I}_{\text{ind}}$ are both off-diagonal, only the case $\delta \neq \alpha$ needs to be considered. Using the geometrical series yields:

$$= \lim_{n\to\infty} \frac{1 - e^{-\beta\frac{(\epsilon_\delta-\epsilon_\alpha)}{n}(n+1)}}{n(1 - e^{-\beta(\epsilon_\delta-\epsilon_\alpha)\frac{1}{n}})} e^{-\beta\epsilon_\alpha} \tag{95}$$

$$= \lim_{n\to\infty} \frac{1 - e^{-\beta\frac{(\epsilon_\delta-\epsilon_\alpha)}{n}(n+1)}}{n(1 - 1 + \beta(\epsilon_\delta-\epsilon_\alpha)\frac{1}{n} + \mathcal{O}(\frac{\beta^2(\epsilon_\delta-\epsilon_\alpha)^2}{n^2}))} e^{-\beta\epsilon_\alpha}. \tag{96}$$

Evaluating the limit $n \to \infty$, one obtains:

$$= \frac{1 - e^{-\beta(\epsilon_\delta-\epsilon_\alpha)}}{\beta(\epsilon_\delta-\epsilon_\alpha)} e^{-\beta\epsilon_\alpha} = \frac{e^{-\beta\epsilon_\alpha} - e^{-\beta\epsilon_\delta}}{\beta(\epsilon_\delta-\epsilon_\alpha)}. \tag{97}$$

(*) becomes:

$$(*) = \frac{1}{Z}\sum_{\alpha\neq\delta}\langle\alpha|\hat{I}_{\text{ind}}|\delta\rangle\langle\delta|\hat{H}_1|\alpha\rangle\frac{e^{-\beta\epsilon_\delta}-e^{-\beta\epsilon_\alpha}}{(\epsilon_\delta-\epsilon_\alpha)} \tag{98}$$

$$= \frac{1}{Z}\sum_{\alpha\neq\delta}\langle\alpha|\hat{I}_{\text{ind}}|\delta\rangle\langle\delta|\hat{H}_1|\alpha\rangle\frac{e^{-\beta\epsilon_\delta}-e^{-\beta\epsilon_\alpha}}{(\epsilon_\delta-\epsilon_\alpha)}. \tag{99}$$

We change our notation, such that k denotes the single momentum states in the wire, whereas d denotes momentum state in the dot:

$$(*) = \frac{1}{Z}\sum_{k}\langle k|\hat{I}_{\text{ind}}|d\rangle\langle d|\hat{H}_1|k\rangle\frac{e^{-\beta\epsilon_d}-e^{-\beta\epsilon_k}}{\epsilon_d-\epsilon_k} + \frac{1}{Z}\sum_{k}\langle d|\hat{I}_{\text{ind}}|k\rangle\langle k|\hat{H}_1|d\rangle\frac{e^{-\beta\epsilon_k}-e^{-\beta\epsilon_d}}{\epsilon_k-\epsilon_d} \tag{100}$$

$$= \frac{1}{Z}2\sum_{k}\langle k|\hat{I}_{\text{ind}}|d\rangle\langle d|\hat{H}_1|k\rangle\frac{e^{-\beta\epsilon_d}-e^{-\beta\epsilon_k}}{\epsilon_d-\epsilon_k}. \tag{101}$$

For reasons of causality, we make an infinitesimal shift of the energy along the positive direction of the imaginary plane [11]. This yields a retarded response function that has no poles in the upper half of the imaginary plane. Its Fourier transform with respect to time: $\epsilon \to (t-t_0)$ yields a Θ-function $\Theta(t-t_0)$. The physical meaning is that the perturbation can only be observed at times $t > t_0$ where t_0 is the time at which the perturbation takes place:

$$(*) = \text{Re}\{\lim_{\eta\to 0} 2\frac{1}{Z}\sum_{k}\langle k|\hat{I}_{\text{ind}}|d\rangle\langle d|\hat{H}_1|k\rangle\frac{e^{-\beta\epsilon_d}-e^{-\beta\epsilon_k}}{\epsilon_d-\epsilon_k+i\eta}\} \tag{102}$$

$$= \text{Re}\{\lim_{\eta\to 0} 2\frac{1}{Z}\sum_{k}\frac{ie\gamma^2}{\hbar}\frac{e^{-\beta\epsilon_d}-e^{-\beta\epsilon_k}}{\epsilon_d-\epsilon_k+i\eta}\}. \tag{103}$$

The sum over k is taken to an integral:

$$\sum_{k,d} \to \int \frac{d\epsilon_k}{2\pi\hbar v_{\text{F}}}, \tag{104}$$

where the density of states $\rho(\epsilon) = \frac{1}{2\pi}\frac{\partial k}{\partial\epsilon_k} = \frac{1}{2\pi\hbar v_{\text{F}}}$ has been introduced. (*) becomes:

$$(*) = \text{Re}\{\lim_{\eta\to 0}\int d\epsilon_k \frac{2}{2\pi\hbar v_{\text{F}}}\frac{ie}{\hbar}\gamma^2\frac{1}{Z}\frac{e^{-\beta\epsilon_d}-e^{-\beta\epsilon_k}}{\epsilon_d-\epsilon_k+i\eta}\}. \tag{105}$$

Since the prefactor contains an imaginary i and in the end, only the real part of the above expression contributes, one can conclude that only the imaginary part of

$\lim_{\eta\to 0}\frac{1}{\epsilon_d-\epsilon_k+i\eta}$ is relevant: $\mathrm{Im}\{\lim_{\eta\to 0}\frac{1}{\epsilon_d-\epsilon_k+i\eta}\}=\pi\delta(\epsilon_d-\epsilon_k)$. This yields:

$$(*)=\int d\epsilon_k\delta(\epsilon_k-\epsilon_d)\frac{2}{2\pi\hbar v_\mathrm{F}}\frac{\pi e}{\hbar}\gamma^2\frac{1}{Z}(e^{-\beta\epsilon_d}-e^{-\beta\epsilon_k}) \tag{106}$$

$$=\int d\epsilon_k\delta(\epsilon_k-\epsilon_d)\frac{2}{2\pi\hbar v_\mathrm{F}}\frac{\pi e}{\hbar}\gamma^2(p_\uparrow^d-p_k^w) \tag{107}$$

where p_k^w denotes the probability for an electron in state k in the wire, i.e. $f(\epsilon_k)$. Eq. (107) yields zero in equilibrium because the population in the dot and in the wire at the corresponding energy are equal. However, this expression illustrates in what way the probabilities enter the equation for the total current. Our goal is to consider the non-equilibrium situation. As far as we analyze the perturbative regime, we can adapt Eq. (106) for our purposes by making the following adaption: We implement a source-drain-configuration by making a spin-dependent shift in chemical potential in the quantum dot which accounts for the different and fixed occupation probabilities for up-spin- and down-spin-electrons in the quantum dot. The substitution $\epsilon_d \xrightarrow{\text{eq.}\to\text{non-eq.}} \epsilon_d+\mu_\sigma$ concerns all thermal factors:

$$\frac{e^{-\beta\epsilon_d}}{Z}\to\frac{e^{-\beta(\epsilon_d+\mu_\sigma)}}{Z},$$

which yields:

$$(*)=\int d\epsilon_k\delta(\epsilon_k-\epsilon_d)\frac{2}{2\pi\hbar v_\mathrm{F}}\frac{\pi e}{\hbar}\gamma^2\frac{1}{Z}(e^{-\beta\epsilon_d+\mu_\uparrow}-e^{-\beta\epsilon_k}) \tag{108}$$

$$=\frac{2}{2\pi\hbar v_\mathrm{F}}\frac{\pi e}{\hbar}\gamma^2\frac{1}{Z}(e^{-\beta\epsilon_d+\mu_\uparrow}-e^{-\beta\epsilon_d})\overset{\gamma=\frac{2\hbar v_\mathrm{F}}{\sqrt{\lambda}}t}{=}4\frac{et^2}{h}\frac{2\pi\hbar v_\mathrm{F}}{\lambda}\frac{1}{Z}(e^{-\beta\epsilon_d+\mu_\uparrow}-e^{-\beta\epsilon_d}) \tag{109}$$

The other term in the brace of Eq. (88) can be treated analogously and will yield the same result with opposite spin and the opposite sign.
Eq. (88) therefore becomes:

$$\langle I\rangle_\mathrm{ind}^\mathrm{neq}=4\frac{et^2}{h}\frac{2\pi\hbar v_\mathrm{F}}{\lambda}\frac{1}{Z}[(e^{-\beta(\epsilon_d+\mu_\uparrow)}-e^{-\beta\epsilon_d})-(e^{-\beta(\epsilon_d+\mu_\downarrow)}-e^{-\beta\epsilon_d})] \tag{110}$$

$$=4\frac{et^2}{h}\frac{2\pi\hbar v_\mathrm{F}}{\lambda}\frac{1}{Z}[e^{-\beta(\epsilon_d+\mu_\uparrow)}-e^{-\beta(\epsilon_d+\mu_\downarrow)}]=4\frac{et^2}{h}\frac{2\pi\hbar v_\mathrm{F}}{\lambda}[p_\uparrow^d-p_\downarrow^d]. \tag{111}$$

Since we have now moved to the nonequilibrium case, $p_\uparrow^d\neq p_\downarrow^d$ will lead to an induced current in the helical wire as is evident from Eq. (111). This equation is general and applicable to different models for the quantum dot.

If one assumes a two-electron quantum dot that can host one electron of each spin state, respectively, the probabilites $p_\uparrow^d$ and $p_\downarrow^d$ are uncorrelated and become

Fermi-Dirac distributions, $f_{QD}(\epsilon_d)$. This is the case that we implemented in Sec. 3.2.
If one assumes strong Coulomb repulsion to allow only a single electron in the dot, the probabilites $p^d_\uparrow$ and $p^d_\downarrow$ are not independent any more. This corresponds to the situation that we considered in Sec. 3.1.

3.3.2 Fermi's Golden Rule

The perturbative ansatz can also be realized by an application of Fermi's Golden Rule that states for the transition rate between the initial state i and the final state f:

$$\Gamma_{i\to f} = \frac{2\pi}{\hbar}\left|\langle i|\hat{H}_T|f\rangle\right|^2\rho(\epsilon_f). \tag{112}$$

where $\rho(\epsilon_f)$ is the DoS in the final state and $\hat{H}_T$ is the tunneling Hamiltonian as introduced above:

$$\hat{H}_T = \gamma\sum_{k,\sigma}(\hat{\Psi}^\dagger_{k,\sigma}\hat{d}_\sigma + h.c.). \tag{113}$$

The following calculation concerns the spin state $\sigma =\uparrow$ which can be treated separately as the two spin states do not mix. We choose the same model for the quantum dot as in the case of the Schrödinger-approach where the quantum dot has two uncorrelated states, one for each spin state. For the tunneling between the wire and the dot, the total rate must be proportional to the Pauli factor: $f_W(\epsilon)(1-f_{QD}(\epsilon))$ where $f(\epsilon)$ denotes the Fermi-Dirac distribution. Evaluating

$$\left|\langle k|\hat{H}_T|d\rangle\right| = \gamma,$$

the total transition rate is given by:

$$\Gamma_{w\to d} = \sum_k \frac{2\pi}{\hbar}\gamma^2\delta(\epsilon_d-\epsilon_k)f_{\mathrm{W}}(\epsilon_k)(1-f_{\mathrm{QD}}(\epsilon_k)). \tag{114}$$

where we chose the low-coupling regime with $\rho(\epsilon_f) = \delta(\epsilon-\epsilon_d)$ in order to be able to compare the result to the one obtained above (see Sec. 3.2). The sum over k is taken to an integral:

$$\sum_k \to \int \frac{d\epsilon_k}{2\pi\hbar v_{\mathrm{F}}}.$$

Consequently,

$$\Gamma_{w\to d} = \int d\epsilon_k \frac{1}{2\pi\hbar v_{\mathrm{F}}}\frac{2\pi}{\hbar}\gamma^2\delta(\epsilon_d-\epsilon_k)f_{\mathrm{W}}(\epsilon_k)(1-f_{\mathrm{QD}}(\epsilon_k)) \tag{115}$$

$$\overset{t=\frac{\gamma\sqrt{\lambda}}{2\hbar v_{\mathrm{F}}}}{=} 4\frac{t^2}{h}\frac{2\pi\hbar v_{\mathrm{F}}}{\lambda}f(\epsilon_d)(1-f(\epsilon_d+\mu_\uparrow)). \tag{116}$$

This, however, is only the transition rate for electrons tunneling from the wire to the dot. The opposite tunneling direction must be taken into account and is computed analogously:

$$\Gamma_{d\to w} = 4\frac{t^2}{h}\frac{2\pi\hbar v_{\mathrm{F}}}{\lambda}f(\epsilon_d+\mu_\uparrow)(1-f(\epsilon_d)). \tag{117}$$

The total tunneling current for spin ↑-electrons is therefore given by:

$$I_T^{\uparrow} = e(\Gamma_{d\to w} - \Gamma_{w\to d}) = 4\frac{t^2}{h}\frac{2\pi\hbar v_{\mathrm{F}}}{\lambda}(f(\epsilon_d + \mu_{\uparrow}) - f(\epsilon_d)). \tag{118}$$

This expression is equivalent to the one that we obtained in the Schrödinger-approach and is a confirmation of the result.

4 Conclusions and Discussion

In this section we aim at interpreting the results that we obtained above. Moreover, we will turn to the physical comparison between our setup and the one by Fillippone and Brouwer that we introduced in Sec. 1.4.

Our comparison is based on the model of the two-electron quantum dot as implemented in the approach via the Schrödinger equation and Fermi's Golden Rule. In this case, both spin states are completely independent which is closest related to the chiral case of Fillippone and Brouwer who consider spinless chiral electrons. The conductance that we have derived in different ways reflects some physical differences to the conductance that Fillippone and Brouwer found. Their tunneling current is independent of the Fermi-Dirac distributions in the wire and in the dot and therefore also independent of temperature in all three regularization choices. This corresponds to a situation where both, the contact and the wire have continuous spectra. Therefore, there is no momentum state in the wire that is "special" and should explicitly appear in the result. In our case, however, the dot only has a single momentum state. It can therefore be expected that the corresponding energy in the quantum dot, which is spin dependently shifted by the chemical potential μ_σ, plays a special role and determines the exact value of the conductance via the dimensionless parameter $\beta(\epsilon_d + \mu_\sigma)$.
Moreover, it is important to note that the system studied in Ref. [5] is a priori symmetric between the contact and the wire. Before specifying the boundary conditions, there is no physical difference between the contact and the wire - both have only one 1D chiral mode and the regularization is symmetric in all three cases, as well. Interchanging the boundary conditions would lead to exactly the same result in the conductance.

This constitutes one of the main differences to our system: The asymmetry between the 1D wire and the 0D quantum dot is evident. This difference in spacial dimensions already hints at the fact that an additional quantity with the dimension of length will appear in the result. We choose this to be λ, the size of the quantum dot. The trivial dependence of the wavefunction on the tunneling parameter t lets us deduce that λ also plays the role of a regularizer. In our case, due to the 0D nature of the quantum dot, an additional regularization is not needed.

Additionally, our system differs from theirs by that fact the our 1D wire is not spinless and chiral but spinfull and helical, meaning that the two different spin states travel in opposite directions. Even if the coupling strength was turned to zero, one could measure a nonzero spin current in the wire.

Since there is a spin-dependent shift in chemical potentials in the dot, the sign of the total current is completely determined by the respective chemical potentials. Contrarily, in the case of Fillippone and Brouwer, the direction of motion of the chiral electrons in the contact and in the dot is a priori determined by the physical system (if the chiral states are taken to be edge states of topologically nontrivial

bulks for example, the topology of the bulk will determine the direction of motion). Because of this relation to the bulk in Ref. [5], the density of states in the contact and in the wire are fixed and do not change by the exchange of electrons. The nontrivial dependence of the conductance on the tunneling parameter t is an artifact of the form of the Schrödinger equation and depends on the regularization choice, even if the density of states is trivial in all cases. The wavefunction in the contact and in the wire already contain this nontrivial t-dependence.
In our setup however, the density of states in the quantum dot can change when it is tunnel coupled to the wire. It depends on the strength of the tunneling junction. This is the reason for the nontrivial dependence on t in our case. The wavefunction in the wire itself has a rather trivial dependence on t which is due to the simpler form of the Schrödinger equation, caused by the fact that the wavefunction in the quantum dot is constant.

Our setup is closely related to the one by Fillippone and Brouwer. By making the necessary physical adaptions, one can merge our result with theirs. We start from our conductance which is valid for small μ_σ, such that a linear response approximation is valid:

$$G_\uparrow = e\frac{I_T^\uparrow}{\mu_\uparrow} = 4\frac{e^2t^2}{h\mu_\uparrow}\frac{2\pi\hbar v_\mathrm{F}}{\lambda}\left(f(\epsilon_d+\mu_\uparrow)-f(\epsilon_d)\right). \tag{119}$$

First, one needs to set $\lambda = 1$ which corresponds to symmetrizing $\hat{H}_T$ since $\lambda = 1$ implies equal dimensions of $\hat{\Psi}(x)$ and $\hat{d}(x)$. Moreover, one needs to change the zero-momentum from the QD to a quasi-continuous spectrum of momenta which requires the integration over $\int \frac{d\epsilon_{d_\uparrow}}{2\pi\hbar v_\mathrm{F}}$ (the DoS in the contact has been intoduced, here):

$$\to G_\uparrow = 4\frac{e^2t^2}{h\mu_\uparrow}2\pi\hbar v_\mathrm{F}\int\frac{d\epsilon_{d_\uparrow}}{2\pi\hbar v_\mathrm{F}}\left(f(\epsilon_d+\mu_\uparrow)-f(\epsilon_d)\right) \tag{120}$$

$$= 4\frac{e^2t^2}{h\mu_\uparrow}\mu_\uparrow = 4\frac{e^2t^2}{h}. \tag{121}$$

which is the result by Fillippone and Brouwer in second order of t [5].

In this thesis, we have only considered helical wires and the question can be raised whether this is a requirement for this spin-to-charge conversion to take place. Phenomenologically, the difference between our setup and the one of a magnetized quantum dot that is tunnel coupled to a regular wire is easy to understand: When an electron of either spin states tunnels from the quantum dot a normal wire, its spin state has no effect on the direction of motion that it will have in the wire since electrons in both spin states can travel in both directions. If the magnetized

quantum dot with spin-dependent shifts in the chemical potential, μ_σ, is interpreted as source that injects electrons into the wire, the magnetization corresponds to an unequal number of injected $\uparrow$- and $\downarrow$-electrons. Because the spin states do not determine the direction of motion in the wire, though, the magnetization of the quantum dot cannot have an effect on the current in the wire which remains zero, irrespective of the magnetization.
On the other hand, the observation of spin-to-charge conversion as described in this thesis is a clear indication that the system is helical.

4.1 Conclusion

In this work, we have investigated the spin-to-charge conversion that can be observed when a quantum dot with different probabilities of hosting $\uparrow$- and $\downarrow$-electrons is tunnel coupled to a helical wire.
We started from phenomenological rate equations which provided an expression for the induced current in the helical wire. We found it to depend on the difference in occupation probabilities for $\uparrow$- and $\downarrow$-electrons in the quantum dot.
Since, due to their phenomenological nature, the rate equations cannot take into account regularization that is necessary for 1D Dirac Fermions, we then turned to a scattering approach in which we explicitly solved the Schrödinger equation. Our calculations show that the nontrivial dependence of the tunneling current on the tunneling parameter t is only due to the broadened density of states of the quantum dot which results from its coupling to the helical wire. We deduced that, due to the 0D nature of the quantum dot, the additional regularization is not needed. The size of the dot plays the role of a regularizer.
In the next step, in order to find a model-independent expression for the spin-to-charge conversion, we used a perturbation theory in the tunneling amplitude. Our result is the following:

$$I_{\text{total}} = 4\frac{et^2}{h}\frac{2\pi\hbar v_{\text{F}}}{\lambda}[p^d_\uparrow - p^d_\downarrow]. \tag{122}$$

This general expression illustrates that the difference in occupation probabilities for $\uparrow$- and $\downarrow$-electrons determines the induced current. The exact expression for the probabilities depends on the model of the quantum dot. In this thesis, we considered it to be either a single-electron quantum dot with strong Coulomb repulsion (in that case, $p^d_\uparrow$ and $p^d_\downarrow$ are correlated) or a quantum dot with two uncorrelated states for $\sigma = \uparrow, \downarrow$. We explained that the observed spin-to-charge conversion is an effect of the helical nature of the 1D quantum wire. Experimentally, this effect can be used for the measurement of spin currents which are otherwise hardly accessible [21].

5 Acknowledgment

I would like to express my gratitude to the LS Delft for the extraordinary working conditions that they provide for their Bachelor students. Moreover, I would like to sincerely thank Oleg Yevtushenko for giving me the opportunity to write this Bachelor's thesis. I appreciated his great mentoring and his constructive technical, as well as personal advice.
Thanks also to Dennis Schimmel who was always available for questions and discussions and offered great support.

References

[1] C. W. J. Beenakker. Colloquium. *Rev. Mod. Phys.*, 80:1337–1354, (2008).

[2] B. Andrei Bernevig and Shou-Cheng Zhang. Quantum Spin Hall Effect. *Phys. Rev. Lett.*, 96:106802, (2006).

[3] M. V. Berry. Quantal Phase Factors Accompanying Adiabatic Changes. *Proceedings of the Royal Society of London A: Mathematical, Physical and Engineering Sciences*, 392(1802):45–57, (1984).

[4] Bernd Braunecker, Pascal Simon, and Daniel Loss. Nuclear Magnetism and Electron Order in Interacting One-Dimensional Conductors. *Phys. Rev. B*, 80:165119, (2009).

[5] Michele Filippone and Piet W. Brouwer. Tunneling into Quantum Wires: Regularization of the Tunneling Hamiltonian and Consistency between Free and Bosonized Fermions. *Phys. Rev. B*, 94:235426, (2016).

[6] David J. Griffiths. *Introduction To Quantum Mechanics*. Pearson Prentice Hall, (2005).

[7] M. Z. Hasan and C. L. Kane. Colloquium. *Rev. Mod. Phys.*, 82:3045–3067, (2010).

[8] Alexander Cyril Hewson. *The Kondo Problem to Heavy Fermions*. Cambridge Studies in Magnetism. Cambridge University Press, (1993).

[9] C. L. Kane and E. J. Mele. $\mathbb{Z}_2$ Topological Order and the Quantum Spin Hall Effect. *Phys Rev Lett*, 95(14):146802, (2005).

[10] C. L. Kane and E. J. Mele. Quantum Spin Hall Effect in Graphene. *Phys. Rev. Lett.*, 95:226801, (2005).

[11] Gerald D. Mahan. *Many-Particle Physics*. Springer Series: Solids and Liquids. Springer, (2000).

[12] Yuli V. Nazarov and Yaroslav M. Blanter. *Quantum Transport: Introduction to Nanoscience*. Cambridge University Press, (2009).

[13] Xiao-Liang Qi and Shou-Cheng Zhang. Topological Insulators and Superconductors. *Rev. Mod. Phys.*, 83:1057–1110, (2011).

[14] C. H. L. Quay, T. L. Hughes, J. A. Sulpizio, L. N. Pfeiffer, K. W. Baldwin, K. W. West, D. Goldhaber-Gordon, and R. de Picciotto. Observation of a One-Dimensional Spin-Orbit Gap in a Quantum Wire. *Nat Phys*, 6(5):336–339, (2010).

[15] Andreas Rank. Tunneling of Electrons between Normal and Helical 1D Wires Coupled via a Quantum Dot. Bachelor's thesis, Ludwig-Maximilians-Universität München, (2017).

[16] Brian K. Ridley. *Quantum Processes in Semiconductors*. Oxford University Press, (1999).

[17] Bruno Rizzo, Alberto Camjayi, and Liliana Arrachea. Transport in Quantum Spin Hall Edges in Contact to a Quantum Dot. *Phys. Rev. B*, 94:125425, (2016).

[18] C. P. Scheller, T.-M. Liu, G. Barak, A. Yacoby, L. N. Pfeiffer, K. W. West, and D. M. Zumbühl. Possible Evidence for Helical Nuclear Spin Order in GaAs Quantum Wires. *Phys. Rev. Lett.*, 112:066801, (2014).

[19] D. H. Schimmel, A. M. Tsvelik, and O. M. Yevtushenko. Low Energy Properties of the Kondo Chain in the RKKY Regime. *New Journal of Physics*, 18(5):053004, (2016).

[20] Shun-Qing Shen. *Topological Insulators - Dirac Equation in Condensed Matters*. Springer Series in Solid-State Sciences, (2012).

[21] Peter Stano and Philippe Jacquod. Spin-to-charge conversion of mesoscopic spin currents. *Phys. Rev. Lett.*, 106:206602, May 2011.

[22] Yoichi Tanaka, A. Furusaki, and K. A. Matveev. Conductance of a Helical Edge Liquid Coupled to a Magnetic Impurity. *Phys. Rev. Lett.*, 106:236402, (2011).

[23] D. J. Thouless, M. Kohmoto, M. P. Nightingale, and M. den Nijs. Quantized Hall Conductance in a Two-Dimensional Periodic Potential. *Phys. Rev. Lett.*, 49:405–408, (1982).

[24] A. M. Tsvelik and O. M. Yevtushenko. Quantum Phase Transition and Protected Ideal Transport in a Kondo Chain. *Phys. Rev. Lett.*, 115:216402, (2015).

[25] Oleg M. Yevtushenko, Ari Wugalter, Vladimir I. Yudson, and Boris L. Altshuler. Transport in Helical Luttinger Liquid with Kondo Impurities. *EPL (Europhysics Letters)*, 112(5):57003, (2015).

[26] Alexandre Zagoskin. *Quantum Theory of Many-Body Systems*. Springer Series: Graduate Texts in Physics. Springer, (2014).

Appendices

A Derivation of the conductance via the Schrödinger equation

The Schrödinger equation for regularization choice (I) reads:

$$0 = -i\hbar v_{\mathrm{F}} \partial_x \Psi_C(x) + \frac{\gamma}{4\delta^2} \int_{-\delta}^{\delta} dx' \Psi_W(x') \tag{123}$$

$$0 = -i\hbar u_{\mathrm{F}} \partial_x \Psi_W(x) + \frac{\gamma}{4\delta^2} \int_{-\delta}^{\delta} dx' \Psi_C(x'). \tag{124}$$

$$\tag{125}$$

where u_{F} and v_{F} denote the Fermi velocity in the wire and in the contact, respectively. One can make a linear ansatz for both wavefunctions:

$$\Psi_C = Ax + B \tag{126}$$

$$\Psi_W = Cx + D. \tag{127}$$

Inserting this into the Schrödiner equation, one obtains the following relations between the parameters:

$$A = \frac{\gamma}{2\delta} \frac{D}{i\hbar v_{\mathrm{F}}} \tag{128}$$

$$C = \frac{\gamma}{2\delta} \frac{B}{i\hbar u_{\mathrm{F}}}. \tag{129}$$

The system can be solved by adding two boundary conditions. If one takes the electron in the contact to be incoming from the left, one can unit the amplitude of the wavefunction at $x = -\delta$ and choose to normalize the wavefunction be the DoS:

$$\Psi_C(-\delta) = \frac{1}{\sqrt{2\pi\hbar v_{\mathrm{F}}}} \tag{130}$$

$$\leftrightarrow A(-\delta) + B = \frac{\gamma}{2\delta} \frac{D}{i\hbar v_{\mathrm{F}}}(-\delta) + B = \frac{1}{\sqrt{2\pi\hbar v_{\mathrm{F}}}}. \tag{131}$$

Moreover, it is convenient to choose the chirality of the wire to allow electrons to travel only from the left to the right (the regularization is independent of the respective chiralities in the contact and in the wire which gives us this freedom of choice.). We can therefore choose the second boundary condition to be:

$$\Psi_W(\delta) = 0 \tag{132}$$

$$\leftrightarrow C\delta + D = \frac{\gamma}{2\delta} \frac{B}{i\hbar u_{\mathrm{F}}} \delta + D = 0. \tag{133}$$

Eqs. (128), (129), (132), and (130) allows us to solve for all four parameters A, B, C and D. Introducing the dimensionless tunnel paramater $t := \frac{\gamma}{2\hbar\sqrt{u_\mathrm{F} v_\mathrm{F}}}$ yields:.

$$\Psi_C(x) = \frac{1}{\sqrt{2\pi\hbar v_\mathrm{F}}} \frac{-t^2 x + \delta}{\delta(1+t^2)} \tag{134}$$

$$\Psi_W(x) = \frac{1}{\sqrt{2\pi\hbar u_\mathrm{F}}} \frac{-it(x+\delta)}{\delta(1+t^2)}. \tag{135}$$

The transmission amplitude is simply:

$$\left|\Psi_W(\delta)\sqrt{2\pi\hbar u_\mathrm{F}}\right|^2 = 4\frac{t^2}{(1+t^2)^2}. \tag{136}$$

which leads to the conductance:

$$G = \frac{e^2}{h}T = 4\frac{e^2 t^2}{h(1+t^2)^2} \overset{t\ll 1}{\approx} 4\frac{e^2 t^2}{h}. \tag{137}$$

B Density of States in QD in the Presence of Tunneling

The effective Hamiltonian for the coupled system reads:

$$\hat{H} = \epsilon_d \hat{d}^\dagger \hat{d} + \sum_k \epsilon_k \hat{\Psi}_k^\dagger \hat{\Psi}_k + \gamma \sum_k (\hat{\Psi}_k^\dagger \hat{d} + \hat{d}^\dagger \hat{\Psi}_k). \tag{138}$$

We use the resolvent Green's function $G(t-t')$:

$$(i\hbar\partial_t - \hat{H})G(t-t') = \delta(t-t') \tag{139}$$

The functions of primary physical interest due to causality are the retarded Green's functions $G^+(t-t')$ which vanishes for $t < t'$ and the advanced Green's function $G^-(t-t')$ which vanishes for $t > t'$. Their Fourier transform is defined as:

$$\to G^\pm(\epsilon) = \int_{-\infty}^{\infty} G^\pm(t-t') e^{-i\epsilon^\pm(t-t')} d(t-t'), \text{ where } \epsilon^\pm = \lim_{s\to 0}(\epsilon \pm is). \tag{140}$$

Thus, Eq. (139) can be rewritten in terms of $G^\pm(t-t')$:

$$(\epsilon^\pm - \hat{H})G^\pm(\epsilon) = \mathbb{1}, \tag{141}$$

which is an operator equation. One can use the eigenstates of Eq. (138) as basis to write this equation componentwise.

$$(\epsilon^\pm - \epsilon_d)G^\pm_{dd}(\epsilon) = \gamma \sum_k G^\pm_{kd}(\epsilon) + 1 \tag{142}$$

$$(\epsilon^\pm - \epsilon_{k'})G^\pm_{k'd}(\epsilon) = \gamma G^\pm_{dd}(\epsilon). \tag{143}$$

This set of equations can be solved for

$$G^{\pm}_{dd}(\epsilon) = \frac{1}{\epsilon^{\pm} - \epsilon_d - \sum_k \frac{\gamma^2}{\epsilon^{\pm} - \epsilon_k}} \overset{\Delta := \sum_k \frac{\gamma^2}{\epsilon^{\pm} - \epsilon_k}}{=} \frac{1}{\epsilon^{\pm} - \epsilon_d - \Delta}. \tag{144}$$

For later purposes, it is useful to define:

$$\Gamma \coloneqq \mathrm{Im}(\Delta). \tag{145}$$

The density of states in the QD, $\mathcal{A}(\epsilon)$, is defined as:

$$\mathcal{A}(\epsilon) = -\frac{1}{\pi}\mathrm{Im}(G^{+}_{dd}(\epsilon)) = -\frac{1}{\pi}\mathrm{Im}(\frac{1}{\epsilon^{+} - \epsilon_d - \Delta}) \tag{146}$$

$$= -\lim_{s\to 0}\frac{1}{\pi}\mathrm{Im}(\frac{1}{\epsilon + is - \epsilon_d - \mathrm{Re}(\Delta) - i\Gamma}) \tag{147}$$

$$= -\lim_{s\to 0}\frac{1}{\pi}\frac{-s-\Gamma}{(\epsilon - \epsilon_d - \mathrm{Re}(\Delta))^2 + (\Gamma^2 + s^2)} = \frac{1}{\pi}\frac{\Gamma}{(\epsilon - \epsilon_d - \mathrm{Re}(\Delta))^2 + \Gamma^2}. \tag{148}$$

$\mathrm{Re}(\Delta)$ is just a homogeneous shift in energy and we can therefore set it to zero. In the next step, Γ needs to be evaluated:

$$\Gamma = \lim_{s\to 0}\sum_k \frac{\gamma^2 s}{(\epsilon - \epsilon_k)^2 + s^2} \overset{\sum_k \to \int \frac{d\epsilon_k}{2\pi\hbar v_{\mathrm{F}}}}{\longrightarrow} \gamma^2 \int d\epsilon_k \delta(\epsilon - \epsilon_k) \underbrace{\frac{1}{2\pi\hbar v_{\mathrm{F}}}}_{\rho_w} \tag{149}$$

$$= \gamma^2 \rho_w. \tag{150}$$

The final expression for the DoS is:

$$\mathcal{A}(\epsilon) = \frac{1}{\pi}\frac{\gamma^2\rho_w}{(\epsilon - \epsilon_d)^2 + (\gamma^2\rho_w)^2} \overset{\gamma = t\frac{2\hbar v_{\mathrm{F}}}{\sqrt{\lambda}}}{=} \frac{1}{\pi}\frac{2t^2\frac{\hbar v_{\mathrm{F}}}{\pi\lambda}}{(\epsilon - \epsilon_d)^2 + (2t^2\frac{\hbar v_{\mathrm{F}}}{\pi\lambda})^2} \tag{151}$$

$$= \frac{1}{\pi}\frac{t^2\frac{1}{\rho_w\pi^2\lambda}}{(\epsilon - \epsilon_d)^2 + (t^2\frac{1}{\rho_w\pi^2\lambda})^2}. \tag{152}$$

C Trotter Formula

The Trotter-Product-Formula for (possibly non-commuting) operators A and B reads: $e^{A+B} = \lim_{N\to\infty}(e^{A/N}\cdot e^{B/N})^N$. Expanding the second exponential to first order yields:

$$e^{A+B} = \lim_{N\to\infty}(e^{A\frac{1}{N}} + e^{A\frac{1}{N}}\frac{B}{N})^N + \mathcal{O}(B^{N+1}) \tag{153}$$

$$= \lim_{N\to\infty}\underbrace{(e^{A\frac{1}{N}} + e^{A\frac{1}{N}}\frac{B}{N})\cdot(e^{A\frac{1}{N}} + e^{A\frac{1}{N}}\frac{B}{N})\cdot\ldots\cdot(e^{A\frac{1}{N}} + e^{A\frac{1}{N}}\frac{B}{N})}_{N\text{factors}} + \mathcal{O}(B^{N+1}). \tag{154}$$

Only terms up to $\mathcal{O}(B)$ are kept:

$$= \lim_{N\to\infty} \left(e^{A} + \sum_{m=1}^{N} e^{A\frac{m}{N}} \frac{B}{N} e^{A\frac{N-m}{N}} \right) + \mathcal{O}(B^2). \tag{155}$$

In our case, the operators are the Hamiltonians $\hat{H}_0$ and $\hat{H}_1$:

$$= \lim_{N\to\infty} \left(e^{-\beta\hat{H}_0} + \sum_{m=1}^{N} e^{-\beta(\hat{H}_0\frac{m}{N})} \frac{-\beta\hat{H}_1}{N} e^{-\beta(\hat{H}_0\frac{N-m}{N})} \right) + \mathcal{O}(\hat{H}_1^2). \tag{156}$$

Since $\hat{H}_1$ is off-diagonal and the expectation value of the current in Eq. (88) also contains the off-diagonal operator $\hat{I}$, the first summand in Eq. (156) will lead to a vanishing contribution. The remaining expression will lead to an even number of operators of each kind in Eq. (88) and therefore survives.

D Electric current in a helical wire without tunneling

The Hamiltonian of a free helical wire is given by:

$$\hat{H}_0 = \hbar v_{\mathrm{F}} \sum_k k(\hat{c}^\dagger_{k,\uparrow}\hat{c}_{k,\uparrow} - \hat{c}^\dagger_{k,\downarrow}\hat{c}_{k,\downarrow})$$

Using $\hat{x} = i\partial_k$, we can express the velocity operator for an electron with momentum k as:

$$\hat{v}_k = \frac{i}{\hbar}[\hat{H}, \hat{x}] = v_{\mathrm{F}}(\hat{c}^\dagger_{k,\uparrow}\hat{c}_{k,\uparrow} - \hat{c}^\dagger_{k,\downarrow}\hat{c}_{k,\downarrow})$$

The mean velocity can be calculated via $\langle\hat{v}\rangle = Tr(\hat{\rho}\hat{v})$ with the density matrix $\hat{\rho} = \sum_{k,\sigma} \hat{c}^\dagger_{k,\sigma}\hat{c}_{k,\sigma}$:

$$\begin{aligned}\langle\hat{v}_k\rangle &= v_{\mathrm{F}} \sum_\sigma \sum_{k,k'} \hat{c}^\dagger_{k,\sigma}\hat{c}_{k,\sigma}(\hat{c}^\dagger_{k',\uparrow}\hat{c}_{k',\uparrow} - \hat{c}^\dagger_{k',\downarrow}\hat{c}_{k',\downarrow}) \\ &= v_{\mathrm{F}} \sum_k (\hat{c}^\dagger_{k,\uparrow}\hat{c}_{k,\uparrow} - \hat{c}^\dagger_{k,\downarrow}\hat{c}_{k,\downarrow})\end{aligned}$$

which leads to the current:

$$\langle\hat{I}\rangle = -e\langle\hat{v}\rangle = -ev_{\mathrm{F}} \sum_k (\hat{c}^\dagger_{k,\uparrow}\hat{c}_{k,\uparrow} - \hat{c}^\dagger_{k,\downarrow}\hat{c}_{k,\downarrow}) = -ev_{\mathrm{F}} \sum_k (\hat{\rho}_{kk,\uparrow} - \hat{\rho}_{kk,\downarrow})$$

Since $\hat{\rho}_{kk,\sigma}$ is spin-independent in equilibrium, we can deduce that, as expected, there is no net current in an unbiased helical wire.

6 Eigenständigkeitserklärung

Hiermit erkläre ich, die vorliegende Arbeit selbständig verfasst zu haben und keine anderen als die in der Arbeit angegebenen Quellen und Hilfsmittel benutzt zu haben.
München, 14. September 2017

Unterschrift